

Non-Innocent Behaviour of Imido Ligands in the Reactions of Silanes with Half-Sandwich Imido Complexes of Nb and V: A Silane/Imido Coupling Route to Compounds with Nonclassical Si–H Interactions

Stanislav K. Ignatov,^[d] Nicholas H. Rees,^[a] Alexei A. Merkoulov,^[c] Stuart R. Dubberley,^[a] Alexei G. Razuvaev,^[d] Philip Mountford,^{*[a]} and Georgii I. Nikonov^{*[b, c]}

Dedicated to Professor M. F. Lappert (FRS) in recognition of his outstanding contributions to organometallic chemistry

Abstract: Reactions of imido complexes $[M(\text{Cp})(=\text{NR}')(\text{PR}'_3)_2]$ ($M = \text{V}, \text{Nb}$) with silanes afford a plethora of products, depending on the nature of the metal, substitution at silicon and nitrogen and the steric properties of the phosphine. The main products are $[M(\text{Cp})(=\text{NR}')(\text{PR}_3)(\text{H})(\text{SiR}_n\text{Cl}_{3-n})]$ ($M = \text{V}, \text{Nb}$; $\text{R}' = 2,6\text{-diisopropylphenyl (Ar)}, 2,6\text{-dimethylphenyl (Ar')}$), $[\text{Nb}(\text{Cp})(=\text{NR}')(\text{PR}'_3)(\text{H})(\text{SiPhR}_2)]$ ($\text{R}_2 = \text{MeH}, \text{H}_2$), $[\text{Nb}(\text{Cp})(=\text{NR}')(\text{PR}'_3)(\text{Cl})(\text{SiHR}_n\text{Cl}_{2-n})]$ and $[\text{Nb}(\text{Cp})(\eta^3\text{-N(R)SiR}_2\text{-H}\cdots)(\text{PR}'_3)(\text{Cl})]$. Complexes with the smaller Ar' substituent at nitrogen react faster, as do more acidic silanes. Bulkier groups at silicon and phosphorus slow down the reaction

substantially. Kinetic NMR experiments supported by DFT calculations reveal an associative mechanism going via an intermediate N-silane adduct $[\text{Nb}(\text{Cp})\{\text{N}(\rightarrow\text{SiHClR}_2)\text{R}'\}(\text{PR}'_3)_2]$ bearing a penta-coordinate silicon centre, which then rearranges into the final products through a Si–H or Si–Cl bond activation process. DFT calculations show that this imido-silane adduct is additionally stabilized by a Si–H \cdots M agostic interaction. Si–H activation is kinetically preferred even when Si–Cl activation affords thermodynamically more stable products. The

niobium complexes $[\text{NbCp}(=\text{NAr})(\text{PMe}_3)(\text{H})(\text{SiR}_2\text{Cl})]$ ($\text{R} = \text{Ph}, \text{Cl}$) are classical according to X-ray studies, but DFT calculations suggest the presence of interligand hypervalent interactions (IHI) in the model complex $[\text{Nb}(\text{Cp})(=\text{NMe})(\text{PMe}_3)(\text{H})(\text{SiMe}_2\text{Cl})]$. The extent of Si–H activation in the $\beta\text{-Si-H}\cdots\text{M}$ agostic complexes $[\text{Cp}\{\eta^3\text{-N(R')SiR}_2\text{-H}\cdots\}\text{M}(\text{PR}'_3)(\text{Cl})]$ ($\text{R}' = \text{PMe}_3, \text{PMe}_2\text{Ph}$) primarily depends on the identity of the ligand *trans* to the Si–H bond. A *trans* phosphine leads to a stronger Si–H bond, manifested by a larger $J(\text{Si-H})$ coupling constant. The Si–H activation diminishes slightly when a less basic phosphine is employed, consistent with decreased back-donation from the metal.

Keywords: agostic bonding • group 5 • hydrides • imido • silicon

[a] Dr. N. H. Rees, Dr. S. R. Dubberley, Prof. P. Mountford
Department of Chemistry, University of Oxford, Chemistry
Research Laboratory, Mansfield Road, Oxford OX1 3TA (UK)
Fax: (+44)8165-272-690
E-mail: philip.mountford@chem.ox.ac.uk

[b] Dr. G. I. Nikonov
Chemistry Department, Brock University
500 Glenridge Ave., St. Catharines, ON, L2S 3 A1 (Canada)
Fax: (+1)905-682-9020
E-mail: gnikonov@brocku.ca

[c] A. A. Merkoulov, Dr. G. I. Nikonov
Department of Chemistry, Moscow State University
Vorob'evy Gory, 119992, Moscow (Russia)

[d] Prof. Dr. S. K. Ignatov, Dr. A. G. Razuvaev
Department of Chemistry, University of Nizhny Novgorod
23 Gagarin Avenue, Nizhny, Novgorod 603950 (Russia)

Supporting information for this article is available on the WWW under <http://www.chemeurj.org/> or from the author.

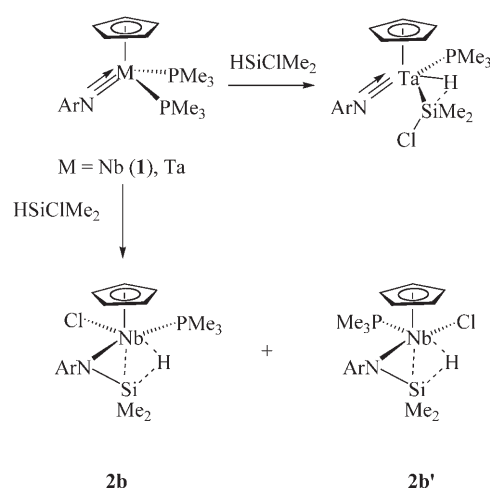
Introduction

The imido-ligand $(\text{RN})^{2-}$ is isolobal with the ubiquitous cyclopentadienyl ligand Cp^- and has been extensively employed for the systematic design of new ligand environments.^[1] For example, Cp/imido, bis(imido) and alkoxyimido ligand sets have been widely used for the preparation of metallocene-like catalysts for olefin polymerization,^[2] dehydrogenative polymerization of silanes^[3] and olefin metathesis.^[4] In addition to its role as a supporting ligand for reactive groups elsewhere in a metal's coordination sphere, such as silyl and hydride ligands,^[3,5] the unsaturated and polar $\text{M}=\text{NR}$ bond itself can act as a potent reaction site towards addition reactions with saturated and unsaturated substrates.^[6]

Despite the extensive chemistry now known for transition metal imido compounds, the direct coupling of silane molecules with $M=NR$ linkages has been little explored. There is significant current interest in the study of metal catalyzed Si–E ($E=C, Si, O, N, S$) bond cleavage/formation processes^[7] with a particular emphasis on Si–C^[8] and Si–O bonds.^[9] However, very little is known about metal mediated Si–N bond formation.^[3g,10] The products of apparent Si–H addition across a $M=N$ multiple bonds have been observed by Tilley et al.^[3g,10a] and Fryzuk et al.^[10c] Silyl group migration from a silylamide ligand to metal to generate a $M=NR$ imido linkage and its reversal, silyl migration from the metal to the imido ligand, have been postulated in only a few cases.^[3g,10b] For the related $M=O$ functionality, silane addition to give a hydride-silyloxy product has been very recently documented for a titanocene complex^[11] and postulated for a rhenium(V)-dioxo catalyst for aldehyde hydrosilylation,^[12] although the latter result was subsequently questioned on the basis of mechanistic studies of a related system.^[13]

Our interest in this field initially stemmed from the desire to extend the study of interligand hypervalent interactions (IHI) $M-H\cdots Si-X$ ($X=F, Cl, Br, I$) in niobocene silyl hydrides to other ligand environments.^[14,15,16] We then turned to the Cp/imido ligand set, which had proved to be isolobal with the Cp_2 ancillary,^[1,17] and found that $[Ta(Cp)(=NAr)(PMe_3)_2]$ ($Ar=2,6$ -diisopropylphenyl) reacted with $HSiClMe_2$ to afford the silylhydrido complex $[Ta(Cp)(=NAr)(SiClMe_2)(H)(PMe_3)]$ with IHI (Scheme 1).^[18] Surprisingly, the reaction of the niobium congener $[Nb(Cp)(=NAr)(PMe_3)_2]$ (**1**) with $HSiMe_2Cl$ gave the β -agostic silylamido compound $[Nb(Cp)\{\eta^3-N(Ar)SiMe_2-H\cdots\}(Cl)(PMe_3)]$ (**2b**) (Scheme 1), a product of Si–N bond formation.^[18,19] In related work, it has been recently found that reactions of the isolobal bis(imido) complex $[Mo(=NAr')_2(PMe_3)_3]$ ($Ar'=2,6$ -dimethylphenyl) with $HSiClMe_2$ and $HSiCl_2Me$ afford only the β -Si–H \cdots Mo agostic complexes $[Mo(=NAr')\{\eta^3-N(Ar')SiMe_2-H\cdots\}(Cl)(PMe_3)_2]$ and $[Mo(=NAr')\{\eta^3-N(Ar')SiMeCl-H\cdots\}(Cl)PMe_3)_2]$.^[20] The latter reactions are rare examples of formal silane addition to a nitrogen based ligand.^[10]

Intrigued by this diversity, we set out to explore in more detail how different factors (in particular the nature of the phosphine, the substitution(s) at silicon and the R group on nitrogen) influence the course of these reactions, the products formed and the extent of any interligand interactions therein.^[21] During these studies, we discovered that in *all* silane addition reactions of the d^2 complexes $[M(Cp)(=NR)(PR'_3)_2]$ ($M=V, Nb, Ta$) the imido ligand demonstrates a surprisingly non-innocent behaviour, with the reactions going via a



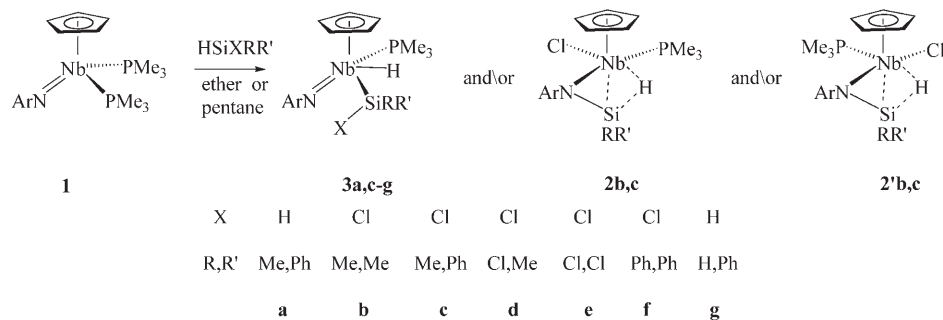
Scheme 1. Reactions of $[M(Cp)(=NAr)(PMe_3)_2]$ ($M=Nb, Ta$) with $HSiClMe_2$.

new silane/imido coupling mechanism. The results of our studies of Nb and V systems are reported herein. Part of this work has been briefly communicated.^[22]

Results and Discussion

The reactions of $[Nb(Cp)(=NAr)(PMe_3)_2]$ (**1**) with silanes:

The reaction between $[Nb(Cp)(=NAr)(PMe_3)_2]$ (**1**) and silanes crucially depends on the identity of substituents at silicon. While **1** reacts with $HSiMe_2Cl$ to give the agostic complexes **2b** and **2b'** as the only observed thermodynamic products (Scheme 1), the analogous reactions of silanes $HSiClR_2$ ($R_2=ClMe, Cl_2, Ph_2$) with more electron-withdrawing R groups at Si lead exclusively to silyl hydride derivatives **3d–f** (Scheme 2).^[23] These compounds were characterized by spectroscopic methods and X-ray structure analyses of **2b**,^[18] **3e**, **3f**^[22] and **3g**. In particular, agostic species give rise to high-field hydride resonances in the 1H NMR spectra in the range -2 to -7 ppm and to low frequency Si–H–Nb bands in the range 1620 – 1670 cm^{-1} , both features are characteristic of complexes with nonclassical Si–H interactions.^[21e] The presence of agostic Si–H \cdots M bonding is con-

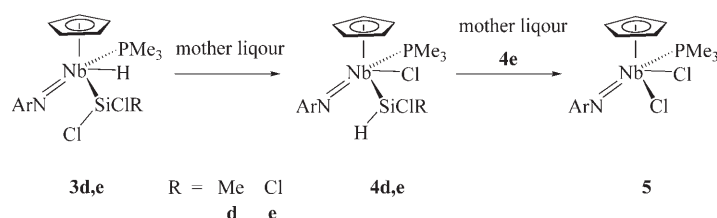


Scheme 2. The interaction of diphosphine complexes **1** with various silanes.

clusively established by the measurement of large H–Si coupling constants (range 96–130 Hz) in the ^{29}Si NMR.^[24] In the ^1H NMR spectra of silyl hydride complexes **3** the hydride resonates in the range 1.65–3.00 ppm, down-field shifted as a result of the anisotropy of the Nb=N bond.^[25] The hydride bands in the IR spectra are observed in the range 1616–1681 cm^{-1} , which is shifted by 50–100 cm^{-1} to a lower frequency, compared with isolobal niobocene complexes.^[26] Unfortunately, the ^{29}Si NMR signals and H–Si coupling constants are not observable in this case^[27] to establish the presence of any nonclassical interaction between the silyl and hydride ligands.

The rate of the reaction in Scheme 2 crucially depends on the Lewis acidity of the silane to be almost instantaneous for HSiCl_3 and to require hours for monochlorosilanes. The chlorine-free silane H_2SiMePh does not react with **1** unless the PMe_3 released is constantly removed from the reaction mixture. Thus, overnight purging of the solution of **1** and H_2SiMePh in toluene with nitrogen gave $[\text{Nb}(\text{Cp})(=\text{NAr})(\text{PMe}_3)(\text{H})(\text{SiHMePh})]$ (**3a**) as a mixture of two diastereomers. In contrast, no reaction occurs upon the addition of HSiMe_2Ph to **1**, even if an overnight purging of nitrogen gas is applied, whereas the more Lewis acidic and smaller silane H_3SiPh reacts with **1** over the course of several minutes, affording the silylhydride **3g**. The reaction of **1** with HSiPh_2Cl is much slower than that with HSiMe_2Cl . It takes four days to achieve 50% conversion in an NMR tube reaction to produce the resultant compound $[\text{Nb}(\text{Cp})(=\text{NAr})(\text{PMe}_3)(\text{H})(\text{SiPh}_2\text{Cl})]$ (**3f**). This compound does not transform into an agostic species, even upon long standing at room temperature. Even the bulkier silane $\text{HSi}i\text{Pr}_2\text{Cl}$ does not react with **1** (in C_6D_6 , hexane, or ether) over the course of several weeks. The silane HSiMePhCl is unique in that both the agostic complex $[\text{Nb}(\text{Cp})(\eta^3\text{-N}(\text{Ar})\text{SiMePh-H}\cdots)(\text{Cl})(\text{PMe}_3)]$ (**2c**) and the silylhydride derivative $[\text{Nb}(\text{Cp})(=\text{NAr})(\text{PMe}_3)(\text{H})(\text{SiPhMeCl})]$ (**3c**) are formed. Both these products were obtained as a mixture of two pairs of diastereomers, owing to the presence of two chiral centres (the metal and the silicon atoms).

The compounds **3d** and **3e** are stable for at least several weeks when isolated from the reaction mixture. However, monitoring the reaction of **1** with HSiMeCl_2 by ^1H NMR reveals that in the mother liquor the initially formed product **3d** transforms into the Cl/H exchange product $[\text{Nb}(\text{Cp})(=\text{NAr})(\text{PMe}_3)(\text{H})(\text{SiHMeCl})]$ (**4d**) over the course of several hours (Scheme 3). The identity of the latter compound was



Scheme 3. Product **3d** is initially formed in the mother liquor and transforms into the Cl/H exchange product **4d** over the course of several hours.

established by spectroscopic methods. In particular, the presence of the SiMeH fragment is supported by the observation in the ^1H NMR spectrum of a Si–H signal at 6.24 ppm (q, $J(\text{H-H}) = 3.3$ Hz) coupled to the methyl group. A Si–H band is seen in the IR spectrum at 2145 cm^{-1} . The compound **3e** slowly decomposes in solution at room temperature in the presence of PMe_3 to give $[\text{Nb}(\text{Cp})(=\text{NAr})(\text{PMe}_3)(\text{Cl})_2]$ (**5**). An intermediate exhibiting a Si–H hydride signal at 7.24 ppm (d, $J(\text{P-H}) = 3$ Hz) and tentatively assigned the rearranged species $[\text{Nb}(\text{Cp})(=\text{NAr})(\text{PMe}_3)(\text{Cl})(\text{SiHCl}_2)]$ (**4e**) was observed in the ^1H NMR spectrum of the reaction mixture kept at room temperature for 18 h.

The X-ray structure of complex $[\text{Nb}(\text{Cp})(=\text{NAr})(\text{PMe}_3)(\text{H})(\text{SiCl}_3)]$ (**3e**) is shown in Figure 1. This compound

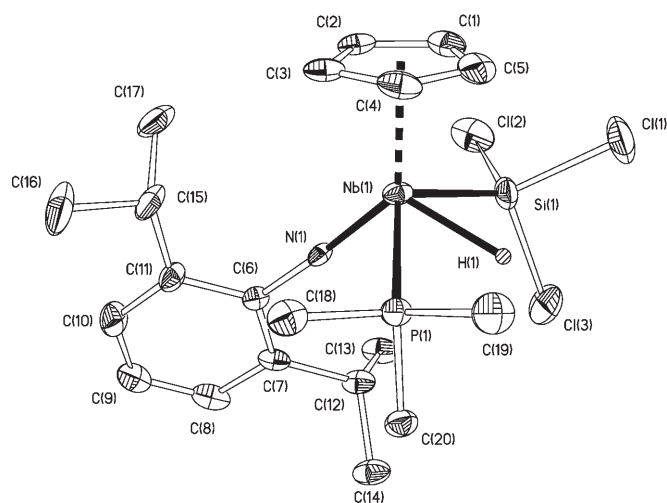


Figure 1. Molecular structure of **3e**. Hydrogen atoms, apart from the hydride, are omitted for clarity. Selected interatomic distances [\AA] and bond angles [$^\circ$]: Nb1–P1 2.534(3), Nb1–Si1 2.541(4), Nb1–N1 1.795(6), Si1–Cl1 2.088(5), Si1–Cl2 2.094(7), Si1–Cl3 2.098(5), Nb1–H1 1.91(4), Si1–H1 2.32, P1–H1 2.39, Nb1–N1–C6 172.7(6), P1–Nb1–Si1 121.98(12), P1–Nb1–N1 88.6(2), Si1–Nb1–N1 98.8(2), Nb1–Si1–Cl1 113.7(3), Nb1–Si1–Cl2 116.05(19), Cl1–Si1–Cl2 104.3(3), Nb1–Si1–Cl3 116.8(2), Cl1–Si1–Cl3 99.1(2), Cl2–Si1–Cl3 104.8(3).

is similar to the previously communicated molecular structure of complex **3f**^[22] and to the tantalum complexes $[\text{Ta}(\text{Cp})(=\text{NAr})(\text{PMe}_3)(\text{H})(\text{SiMe}_{3-n}\text{Cl}_n)]$ ($n = 1, 2$).^[18,28] The Nb–Si bond length of 2.541(4) \AA is close to the Nb–Si bonds in $[\text{Nb}(\text{Cp})_2(\text{SiCl}_3)_2(\text{H})]$ (2.5597(5) and 2.5776(5) \AA).^[29] Unlike $[\text{Ta}(\text{Cp})(=\text{NAr})(\text{PMe}_3)(\text{H})(\text{SiMeCl}_2)]$ ^[28] and the isolobal titanium complex $[\text{Ti}(\text{Cp})_2(\text{SiCl}_3)(\text{H})(\text{PMe}_3)]$,^[15] there are no significant differences in the Si–Cl bond lengths within the trichlorosilyl group (a narrow range of 2.088(5)–2.098(5) \AA is observed), which indicates the absence of any interligand hypervalent Si–H interaction.^[14–16,28,30] The same conclusion applies to complex **3f**^[22] and the isolobal niobocene species $[\text{Nb}(\text{Cp})_2(\text{SiCl}_3)_2(\text{H})]$.^[29] Such lack of IHI can be ascribed either to the diminished basicity of the hydride or to increased hyperconjugation between the chloride lone pairs and the $\sigma^*(\text{Si-Cl})$ antibonding orbital of the chlorine atom lying

trans to the hydride.^[22,29] However, the latter explanation appears to be less likely in light of the nonclassical structure of $[\text{Ti}(\text{Cp})_2(\text{SiCl}_3)(\text{H})(\text{PMe}_3)]$, which featured Si–Cl distances of 2.1606(14) (Si–Cl *trans* to Ti–H), 2.1090(14) and 2.1036(12) Å.^[15]

The X-ray structure of complex $[\text{Nb}(\text{Cp})(=\text{NAr})(\text{PMe}_3)(\text{H})(\text{SiPhH}_2)]$ (**3g**) is shown in Figure 2. Compared with the related compounds **3e** and **3f**, the Nb–Si bond of 2.591(1) Å is elongated due to the weaker electron-withdrawing nature of substituents at silicon. In classical niobium silyl complexes, the Nb–Si bond lengths fall in the range 2.624–2.669(1) Å.^[26,31]

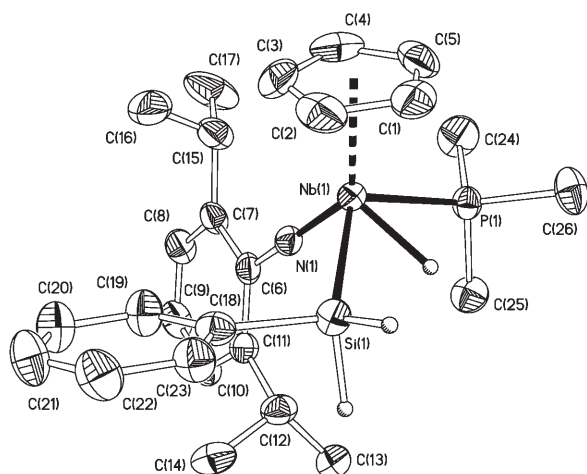
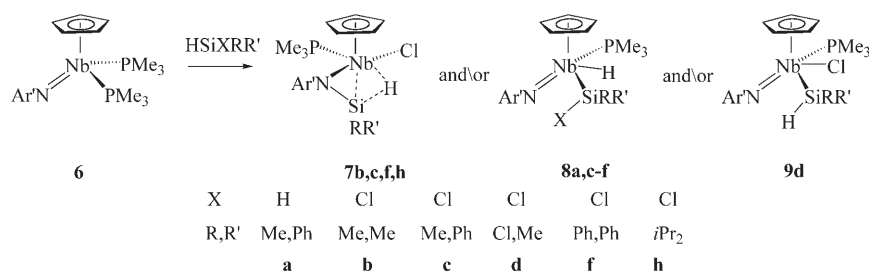


Figure 2. Molecular structure of **3g**. Hydrogen atoms, apart from the hydride, are omitted for clarity. Selected interatomic distances [Å] and bond angles [°]: Nb1–N1 1.816(3), Nb1–P1 2.5236(9), Nb1–Si1 2.5908(10), Si1–C18 1.900(3), Nb1–H 1.74(3), Si1–H27 1.34(5), Si1–H28 1.54(4), N1–Nb1–P1 89.45(8), N1–Nb1–Si1 97.66(8), C18–Si1–H27 104.5(18), C18–Si1–H28 99.5(14), Nb1–Si1–C18 114.92(10), Nb1–Si1–H27 120.4(19), Nb1–Si1–H28 116.3(13), H27–Si1–H28 98(2).

The reactions of $[\text{Nb}(\text{Cp})(=\text{NAr})(\text{PMe}_3)_2]$ with silanes: Reactions of less sterically encumbered diphosphine precursors $[\text{Nb}(\text{Cp})(=\text{NAr})(\text{PMe}_3)_2]$ (**6**) ($\text{Ar}' = 2,6$ -dimethylphenyl) with silanes (Scheme 4) afford the same types of products, but are much faster than in the case of Ar-substituted series **3a,c-f** and **2b,c**. The reaction of **6** with HSiMe_2Cl gives only one isomer of the agostic compound $[\text{Nb}(\text{Cp})\{\eta^3\text{-N}(\text{Ar}')\text{SiMe}_2\text{-H}\cdots\}(\text{Cl})(\text{PMe}_3)]$ (**7b**, PMe_3 *trans* to H) within



Scheme 4. The reactions of less sterically encumbered diphosphine precursors with silanes.

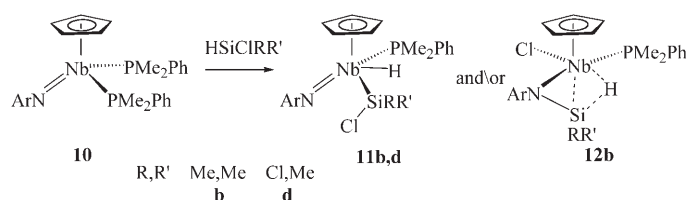
5–8 min.^[18] An analogous reaction with the bulkier silane HSiMePhCl occurred within 35 min to give the β -agostic compound $[\text{Nb}(\text{Cp})\{\eta^3\text{-N}(\text{Ar}')\text{SiMePh-H}\cdots\}(\text{Cl})(\text{PMe}_3)]$ (**7c**) as a mixture of two diastereomers that differed in the orientation of the Ph or the Me group at Si. One of these isomers is predominant (95% yield), but the exact stereochemistry could not be established. On heating at 60°C, these isomers do not interconvert, but rather decompose into two unidentified products.

In contrast to the case for $[\text{Nb}(\text{Cp})(=\text{NAr})(\text{PMe}_3)_2]$ (Scheme 2), the reaction of **6** with HSiPh_2Cl gives not only the silylhydride product $[\text{Nb}(\text{Cp})(=\text{NAr})(\text{PMe}_3)(\text{H})(\text{SiPh}_2\text{Cl})]$ (**8f**) but also (in about 20% yield) the β -agostic compound $[\text{Nb}(\text{Cp})\{\eta^3\text{-N}(\text{Ar}')\text{SiPh}_2\text{-H}\cdots\}(\text{Cl})(\text{PMe}_3)]$ (**7f**). Compound **7f**, which was isolated and fully characterized, shows a characteristic higher-field-shifted Cp signal at 4.79 ppm and a hydride signal at –2.45 ppm in its ¹H NMR spectrum. The reaction of $[\text{Nb}(\text{Cp})(=\text{NAr})(\text{PMe}_3)_2]$ with H_2SiMePh cleanly gives two diastereomers of the silylhydride $[\text{Nb}(\text{Cp})(=\text{NAr})(\text{PMe}_3)(\text{H})(\text{SiPhMeH})]$ (**8a**).

An NMR tube scale reaction of **6** with HSiMeCl_2 gives a complex reaction mixture in which the signals of the main components, $[\text{Nb}(\text{Cp})(=\text{NAr})(\text{PMe}_3)(\text{H})(\text{SiMeCl}_2)]$ (**8d**) and $[\text{Nb}(\text{Cp})(=\text{NAr})(\text{PMe}_3)(\text{Cl})(\text{SiMeHCl})]$ (**9d**), are seen in approximate 1:1 ratio. Interestingly, a minor set of resonances attributable to the β -agostic product $[\text{Nb}(\text{Cp})\{\eta^3\text{-N}(\text{Ar}')\text{SiMeCl-H}\cdots\}(\text{Cl})(\text{PMe}_3)]$ was also observed; a Cp signal at 4.74 ppm and Si–H \cdots Nb hydride signal at –2.96 (d, $J(\text{P-H}) = 12$ Hz). An NMR tube scale reaction of **6** with HSiCl_3 afforded a complex reaction mixture that contained $[\text{Nb}(\text{Cp})(=\text{NAr})(\text{PMe}_3)(\text{H})(\text{SiCl}_3)]$ (**8e**) as well as a range of uncharacterized products. A preparative scale reaction was not attempted.

In contrast to the case for **1**, the compound $[\text{Nb}(\text{Cp})(=\text{NAr})(\text{PMe}_3)_2]$ does react slowly with HSiPr_2Cl , producing the agostic compound $[\text{Nb}(\text{Cp})\{\eta^3\text{-N}(\text{Ar}')\text{SiPr}_2\text{-H}\cdots\}(\text{Cl})(\text{PMe}_3)]$ (**7h**) characterized by a Cp signal at 4.78 ppm and the up-field Si–H \cdots Nb signal at –3.89 ppm. The reaction was 17% complete overnight and about 50% complete after 4 days, based on integration of the Cp region. Unfortunately, attempted preparative scale reactions also produced inseparable side-products, which hampered the isolation of the product.

The reactions of $[\text{Nb}(\text{Cp})(=\text{NR})(\text{PPhMe}_2)_2]$ with silanes: To determine the effect of phosphine substituents, a new diphosphine complex $[\text{Nb}(\text{Cp})(=\text{NR})(\text{PPhMe}_2)_2]$ (**10**) was prepared and its reactions with silanes were studied (Scheme 5). A 1:1 reaction of **10** with HSiMe_2Cl gives a mixture of compounds $[\text{Nb}(\text{Cp})(=\text{NR})(\text{PPhMe}_2)(\text{H})(\text{SiMe}_2\text{Cl})]$ (**11b**) and $[\text{Nb}(\text{Cp})\{\eta^3\text{-N}(\text{Ar}')\text{SiMe}_2\text{-H}\cdots\}(\text{Cl})(\text{PPhMe}_2)]$ (**12b**) and is



Scheme 5. A study of the reactions of silanes with the diphosphine complex **10**.

significantly slower than the analogous reaction of **1**. Thus, after 29 h the ratio of **10**:**11b**:**12b** was 30:3:1, which changed to 7:1:1 after 4.5 days. A preparative scale reaction gave a mixture in which the agostic complex **12b** was the major component along with some amount of $[\text{Nb}(\text{Cp})(=\text{NAr})(\text{PPhMe}_2)(\text{H})(\text{SiMe}_2\text{Cl})]$ (**11b**).

The reaction of **10** with HSiMeCl_2 also proceeds more slowly (about 15 h in an NMR tube experiment) than the analogous reaction of **1**. The conversion of the initial product **11d** into the rearranged species $[\text{Nb}(\text{Cp})(=\text{NAr})(\text{PPhMe}_2)(\text{Cl})(\text{SiMeHCl})]$ (**13d**) is so sluggish that it takes weeks for completion. A preparative scale synthesis of **13d** required four weeks, affording compound **13d** in 12% yield.

The reaction of the 2,6-dimethylphenyl imido analogue $[\text{Nb}(\text{Cp})(=\text{NAr}')(\text{PPhMe}_2)_2]$ (**14**) with HSiMe_2Cl afforded the β -agostic species $[\text{Nb}(\text{Cp})\{\eta^3\text{-N}(\text{Ar}')\text{SiMe}_2\text{-H}\}\text{(Cl)}(\text{PMe}_2\text{Ph})]$ (**15b**) in 36% isolated yield. Compound **15b** was characterized by spectroscopic methods and X-ray diffraction (Figure 3). The hydride ligand position was not determined. The structure of **15b** is very similar to that previously determined for $[\text{Nb}(\text{Cp})\{\eta^3\text{-N}(\text{Ar}')\text{SiMe}_2\text{-H}\}\text{(Cl)}(\text{PMe}_3)]$ (**7b**)^[18,32] and, as the latter, features the phosphine ligand

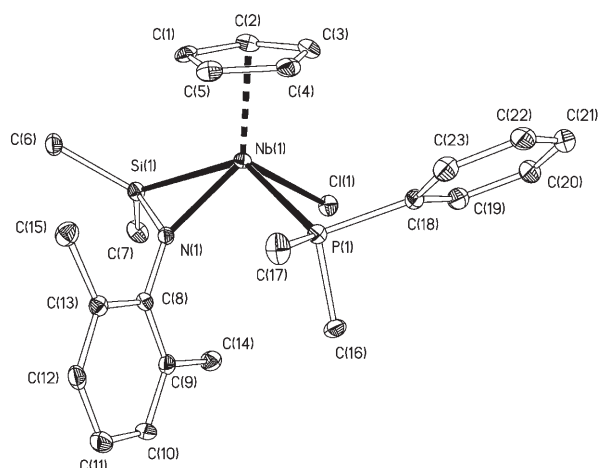


Figure 3. Molecular structure of **15b**. Hydrogen atoms are omitted for clarity. Hydride atom has not been determined. Selected bond distances [Å] and bond angles [°]: Nb1–N1 2.057(3), Nb1–Cl1 2.4831(11), Nb1–P1 2.5966(13), Nb1–Si1 2.6794(12), Si1–N1 1.720(3), Si1–C6 1.867(5), Si1–C7 1.865(4), N1–Nb1–P1 93.57(10), N1–Nb1–Cl1 101.12(9), N1–Nb1–Si1 39.93(9), Cl1–Nb1–Si1 96.69(4), P1–Nb1–Si1 132.95(4), N1–Si1–C6 117.3(2), N1–Si1–C7 119.1(2), C6–Si1–C7 108.5(2), N1–Si1–Nb1 50.15(11), C6–Si1–Nb1 119.04(17), C7–Si1–Nb1 130.05(17), Nb1–N1–Si1 89.93(15).

trans to the agostic Si–H bond. The Nb–Si distance of 2.6794(12) Å in **15b** is slightly longer than that in the related complex $[\text{Nb}(\text{Cp})\{\eta^3\text{-N}(\text{Ar})\text{SiMe}_2\text{-H}\}\text{(Cl)}(\text{PMe}_3)]$ (**2b**, 2.646(1) Å), which has a chloride ligand *trans* to the Si–H bond.^[18] The difference in geometry corresponds well to the difference in the Si–H coupling constant in **15b** and **2b**; the *trans* phosphine induces a larger $J(\text{H-Si})$ (132 Hz in **15b** versus 96 Hz in **2b**) and, presumably, stronger Si–H interaction. It is interesting that in the isomers having chloride *trans* to hydride the variation of phosphine does not significantly affect the degree of Si–H...M agostic bonding. Thus, the $J(\text{H-Si})$ of 96 Hz in Cl-*trans* $[\text{Nb}(\text{Cp})\{\eta^3\text{-N}(\text{Ar})\text{SiMe}_2\text{-H}\}\text{(Cl)}(\text{PMe}_3)]$ (**2b**) is comparable with the $J(\text{H-Si}) = 100$ Hz in Cl-*trans* $[\text{Nb}(\text{Cp})\{\eta^3\text{-N}(\text{Ar})\text{SiMe}_2\text{-H}\}\text{(Cl)}(\text{PMe}_2\text{Ph})]$ (**12b**). Therefore, we can conclude that it is mainly the *trans*-influence of the ligand *trans* to the Si–H...M moiety that controls the extent of Si–H addition to metal.

Reactions of $[\text{VCp}(=\text{NAr})(\text{PMe}_3)_2]$ with chlorosilanes: In contrast to its heavier Group 5 congeners, the vanadium complex $[\text{VCp}(=\text{NAr})(\text{PMe}_3)_2]$ ^[33] does not react with HSiMe_2Cl over the course of several days. Even after heating to 60 °C for an hour, there was no sign of reaction. In contrast, the reaction with HSiMeCl_2 is fast and complete within 30 min, the spectroscopic features of the initial product are consistent with its formulation as a silyl hydride $[\text{VCp}(=\text{NAr})(\text{PMe}_3)(\text{H})(\text{SiMeCl}_2)]$ (**16**). This product, however, is unstable at room temperature and decomposes into the known paramagnetic compound $[\text{VCp}(\text{PMe}_3)_2(\text{Cl})_2]$,^[34] whose identity was established by X-ray diffraction analysis. The reaction of $[\text{VCp}(=\text{NAr})(\text{PMe}_3)_2]$ with HSiCl_3 gave a mixture of products.

Mechanism of silane addition: The experimental data presented above clearly establish that reactions of complexes $[\text{MCp}(=\text{NR})(\text{PR}'_3)_2]$ (M = V, Nb) with silanes **a-h** depend on the identity of the metal, the substituent R at nitrogen, the phosphine PR'_3 and the nature of the silane itself. Apart from the Lewis acidity of the silane, steric considerations appear to be the key factors controlling the rate of these reactions. In the Ar-substituted niobium compounds **1** and **10**, the reactions of the PMe_3 derivatives with ClHSiMe_2 occur within a few hours, whereas several days are required in the case of complexes with the bulkier phosphine PPhMe_2 . In contrast, with the smaller imido N-substituent Ar', the reactions are fast both for the PMe_3 and PPhMe_2 homologues. In fact, there appears to be an inverse correlation between the basicity of the phosphine and the rate of the reaction (complexes with the more basic PMe_3 react faster), and therefore phosphine elimination is unlikely to be rate-determining. The bulky silane ClHSiPr_2 does not react with $[\text{Nb}(\text{Cp})(=\text{NAr})(\text{PMe}_3)_2]$, but a slow reaction with $[\text{Nb}(\text{Cp})(=\text{NAr}')(\text{PMe}_3)_2]$ was observed in an NMR tube experiment. The same sensitivity to steric factors is seen in the lack of reaction between the vanadium diphosphine complex $[\text{V}(\text{Cp})(=\text{NAr})(\text{PMe}_3)_2]$ and HSiMe_2Cl . These observations

are in accord with an associative mechanism, in which the addition of silane precedes the elimination of phosphine. The fact that more Lewis acidic silanes react much faster also supports an associative mechanism (*vide infra*). Finally, an important observation is that all rearrangement reactions of the initially formed products are significantly accelerated in the presence of phosphines. This suggests that a diphosphine species participates in the rearrangement even though both the starting compound and product(s) contain only one phosphine ligand.

To gain an insight into the mechanism of formation of the β -agostic complex **2b**, a set of ^1H variable temperature NMR investigations of the reaction of $[\text{Nb}(\text{Cp})(=\text{NAr})(\text{PMe}_3)_2]$ (**1**) with HSiMe_2Cl were carried out. Addition of a ten-fold excess of silane to **1** gives a mixture of the agostic complex **2b** and a new compound **3b**, whose spectral features are very close to those of the tantalum complex $[\text{Ta}(\text{Cp})(=\text{NAr})(\text{PMe}_3)(\text{H})(\text{SiMe}_2\text{Cl})]$.^[18] Based on this analogy, this new product was assigned the structure $[\text{Nb}(\text{Cp})(=\text{NAr})(\text{PMe}_3)(\text{H})(\text{SiMe}_2\text{Cl})]$ (**3b**). In an hour, the ratio of **2b** to **3b** was about 1:1, with almost all of the **1** consumed. Complex **3b** is a kinetic product of the reaction and, if kept in mother liquor at room temperature, transforms during several hours into the thermodynamically more stable product **2b**. No signals for the possible "rearranged product" $[\text{Nb}(\text{Cp})(=\text{NAr})(\text{PMe}_3)(\text{Cl})(\text{SiMe}_2\text{H})]$ were observed in the reaction mixture. A spin saturation transfer experiment revealed that all the key species (**1**, **2b**, and **3b**) present in the reaction mixture were in equilibrium.

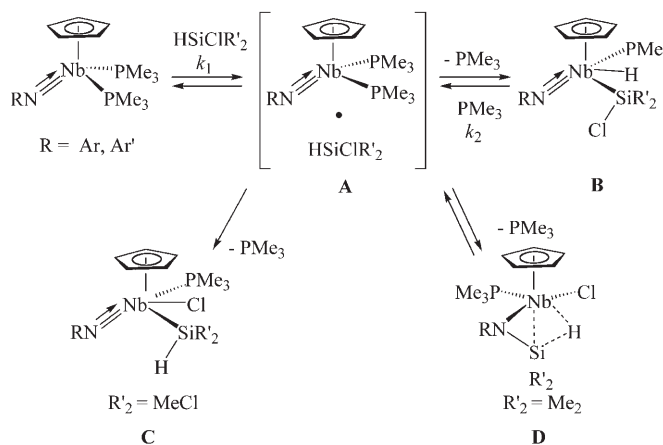
If excess silane HSiMe_2Cl (about twenty equivalents) is used, the decay of **1** at the early stage of reaction (≈ 40 – 50 min) follows pseudo-first-order kinetics with $k_1(21.5^\circ\text{C}) = 9.8(4) \times 10^{-2} \text{ min}^{-1}$. Studying the reaction in the temperature range -10 to $+22^\circ\text{C}$ allowed us to estimate the activation parameters as $\Delta H^\ddagger = 9.7$ (1.2) kcal mol^{-1} and $\Delta S^\ddagger = -29.9(4.4) \text{ cal mol}^{-1} \text{ K}^{-1}$. The negative entropy of activation suggests an associative mechanism and rules out phosphine elimination from **2** in the rate-determining step. During the reaction, the decay of **1** slows as the concentration of PMe_3 increases, and addition of excess PMe_3 slows the reaction significantly. Moreover, addition of phosphine either to **2b** or to a 1:1 mixture of **2b** and **3b** leads to the formation of **1**, in accord with the presence of an equilibrium.

After most of the **1** has been consumed, the decay of **3b** at the early stage of reaction (4–5 h) follows pseudo-first order kinetics with the $k_2(20.5^\circ\text{C})$ of $2.01(7) \times 10^{-3} \text{ min}^{-1}$ (in the presence of about 25 equivalents of HSiMe_2Cl and about 2 equivalents of PMe_3). Studying the reaction in the temperature range $+10$ to $+30^\circ\text{C}$ gave an estimation of the activation parameters as $\Delta H^\ddagger = 9.3(1.4) \text{ kcal mol}^{-1}$ and $\Delta S^\ddagger = -39.6(4.9) \text{ cal mol}^{-1} \text{ K}^{-1}$. The negative entropy of activation indicates an associative mechanism for the transformation of **3b** to **2b**. When all the volatiles have been pumped off and the residue is re-dissolved in fresh C_6D_6 , the rate of reaction decreases by an order of magnitude to $k_2(20^\circ\text{C}) = 1.28(5) \times 10^{-4} \text{ min}^{-1}$. After 3 equivalents of PMe_3 have been added, the k_2 increases again to $7.7(2) \times$

10^{-3} min^{-1} at 29°C . These kinetic studies, although obscured by the equilibrium between **1**, **2b** and **3b**, establish that free PMe_3 is required to facilitate the conversion of **3b** into **2b**. Since both complexes contain only one phosphine ligand, the PMe_3 is the catalyst of this reaction, once again suggesting an associative mechanism.

Similar observations have been made for the rearrangement of $[\text{Nb}(\text{Cp})(=\text{NAr})(\text{PMe}_3)(\text{H})(\text{SiMeCl}_2)]$ (**3d**) into the chloride silyl complex $[\text{Nb}(\text{Cp})(=\text{NAr})(\text{PMe}_3)(\text{Cl})(\text{SiHMeCl})]$ (**4d**). Pure **3d** is stable in C_6D_6 solutions at least for several days. Addition of 12 equivalents of PMe_3 causes the formation of a 3:1 mixture of **4d** and **3d** contaminated by some minor co-products. When a large excess of PMe_3 is added, the main decomposition product is the known paramagnetic compound $[\text{Nb}(\text{Cp})(\text{PMe}_3)_3(\text{Cl})_2]$ ^[35] isolated in the form of red crystals and characterized by an X-ray diffraction study.

Altogether, these data suggest an associative mechanism for the interactions of **1** with silanes (Scheme 6). The key intermediate, schematically shown as **A**, is an adduct of **1** with



Scheme 6. Mechanism of the interaction of diphosphine complexes **1** and **6** with silanes.

silane, containing two phosphine ligands. Its structure will be discussed in more detail in the next section. Decomposition of this complex either by Si–H or Si–Cl bond activation leads to compounds **B**, **C**, or **D**. For $\text{M}=\text{Nb}$ the product of Si–H bond activation, compound **B**, is formed as a kinetic product in reactions with HSiMe_2Cl , HSiMeCl_2 , and HSiCl_3 and as a thermodynamic product in the case of HSiPh_2Cl . Complex **C** is the final product in the reaction with HSiCl_2Me , but no such product can be observed in the case for HSiClMe_2 . Complex $[\text{Nb}(\text{Cp})(=\text{NAr})(\text{PMe}_3)(\text{H})(\text{SiCl}_3)]$ (**3e**) is more inert than $[\text{Nb}(\text{Cp})(=\text{NAr})(\text{PMe}_3)(\text{H})(\text{SiMeCl}_2)]$ (**3d**) but in the presence of phosphine it also transforms to give the compound $[\text{Nb}(\text{Cp})(=\text{NAr})(\text{PMe}_3)(\text{Cl})_2]$ (**5**), the product of formal extrusion of silylene, SiHCl .

Based on the results of these kinetic studies, we have eventually succeeded in the preparation of the elusive com-

plex $[\text{Nb}(\text{Cp})(=\text{NAr})(\text{PMe}_3)(\text{H})(\text{SiMe}_2\text{Cl})]$ (**3b**). The reaction between $[\text{Nb}(\text{Cp})(=\text{NAr})(\text{PMe}_3)_2]$ (**1**) and HSiMe_2Cl was performed in pentane at room temperature. After 1.5 h the solution was concentrated in vacuo to produce a light yellow powder of **3b** in about 9% isolated yield. Pure complex **3b** is stable in solution in the absence of PMe_3 at least for several hours, allowing for its characterization by spectroscopic methods.

Finally, it should be noted the idea of E–H bond (E = group 14 element) activation on the imido ligand is not quite new. Wolczanski et al.^[36] and Bergman et al.^[37] documented C–H bond cleavage by early transition metal d⁰ imido complexes, for which oxidative addition pathway is not feasible. However, these reactions are believed to proceed through an initial electrophilic C–H activation on the metal centre.^[36d] In contrast, our complexes $[\text{M}(\text{Cp})(=\text{NR})(\text{PR}'_3)_2]$ (M = Group 5 metal) are co-ordinatively saturated and the Si–H activation process is different in that it proceeds through an initial nucleophilic addition of electron-rich imido nitrogen atom to the silicon atom.

DFT study of the mechanism of silane–imido coupling: To gain an insight into the structure of complexes **A–D** in Scheme 6 and to establish their relative stability, we carried out DFT calculations on model niobium complexes **17–27** (Tables 1 and 2, Figures 4, 5 and 6). For computational sim-

Table 1. Relative energies (ΔE) and selected interatomic distances [\AA] in structures **18–23**.

	Structures					
	18	19-cis	19	20	21	23
ΔE ^[a]	11.0 ^[b]	3.6	1.4	0.0	6.0	11.4
Nb–H*	1.943	1.793	1.811	2.052	3.378	1.765
Nb–N	1.998	1.793	1.792	2.034	1.784	2.012
Nb–P4, P5	2.587, 2.552	2.535	2.542	2.571	2.638	2.512
Nb–Si	2.909	2.587	2.576	2.746	2.664	3.512
Nb–Cl	4.465	3.904	3.875	2.515	2.566	4.820
Si–N	1.806	3.083	3.134	1.730	3.057	1.731
Si–H*	1.607	2.075	2.035	1.556	1.500	3.458
Si–Cl	2.446	2.149	2.171	3.885	3.127	2.116

[a] [kcal mol^{-1}]; [b] The energy of free PMe_3 is subtracted.

Table 2. Relative energies (ΔE) and selected interatomic distances [\AA] in structures **17, 22–27**.

	Structures					
	17 ^[a]	22 ^[a,b]	24	25 ^[b]	26 ^[b]	27 ^[b]
ΔE ^[c]			9.35	0.62	9.34	0.00
Nb–H*	–	–	1.928	1.806	2.218	–
Nb–N	1.824	1.797	1.995	1.789	2.031	1.782
Nb–P4, P5	2.521, 2.536	2.521	2.552, 2.579	2.541	2.549	2.632
Nb–Si	–	–	2.901	2.551	2.792	2.672
Nb–Cl	–	–	–	–	2.508	2.572
Si–N	–	–	1.786	–	1.724	–
Si–H*	–	–	1.609	2.052	1.507	1.494
Si–Cl	–	–	2.289, 2.152	2.144, 2.124	2.100	2.154

[a] The energy of free HSiCl_2Me is added; [b] the energy of free PMe_3 is added; [c] [kcal mol^{-1}]; [d] 4.9 kcal mol^{-1} relatively **20**, 10.4 kcal mol^{-1} relatively **27**; [e] 41.2 kcal mol^{-1} relatively **20**; 46.7 kcal mol^{-1} relatively **27**.

plicity a methyl substituent at nitrogen was used instead of aryl groups. There is a very good agreement between the calculated and observed geometries, when the latter are available from X-ray analyses.

In accord with our experimental findings, the most thermodynamically favourable product on the electronic energy scale is the agostic compound **20**, the silylhydride **19** is only 1.4 kcal mol^{-1} less stable (Figure 4). The order is, however, reversed on the Gibbs energy scale ($-1.7 \text{ kcal mol}^{-1}$). In both cases the difference is at the limits of accuracy of our calculations. An isomer of **19**, the complex **19-cis**, having a methyl group at silicon *trans* to hydride, is further destabilized by 2.2 kcal mol^{-1} . The least stable product is the “re-arranged” complex **21**, which accounts for our failure to observe it experimentally.

We have considered two reaction pathways for the formation of complexes **19, 20**, and **21**: i) dissociative, proceeding through phosphine elimination from **17** to give the monophosphine complex **22** followed by silane addition to produce **19** (Figure 4), and ii) an associative one, going via a penta-coordinate silicon compound **18**. The latter complex serves as a model for the proposed key intermediate **A** discussed above in Scheme 6. The dissociative mechanism is strongly disfavoured on the electronic energy scale (complex **22** lies 30.2 kcal mol^{-1} above **18**), but becomes competitive with the associative mechanism on the free energy scale (Figure 4). It should be noted that the potential energy surface (PES) around intermediate **22** is very shallow so that the transition state **TS**₁₇₋₂₂ stands out from the intermediate **22** by merely 1 kcal mol^{-1} and thus, can be characterized as a “loose” transition state.^[38,39] Phosphine elimination from **17** via **TS**₁₇₋₂₂, however, is much less favourable on the Gibbs free energy scale (33.1 kcal mol^{-1}).

Addition of HSiMe_2Cl to the imido group of diphosphine **17** to give complex **18** goes via the transition state **TS**₁₇₋₁₈ which requires a significant barrier of 33.9 kcal mol^{-1} (free energy scale), which is close (within the accuracy of our calculations) to the **TS**₁₇₋₂₂. An interesting feature of complex **18** is that it contains a penta-coordinate silicon centre interacting with the metal through agostic Si–H \cdots M bonding (vide infra).

We also searched for an alternative associative mechanism based on direct silane attack on the metal of **17** to give a η^1 -silane complex $[\text{Cp}(\text{MeN})\text{Nb}(\eta^1\text{-HSiMe}_2\text{Cl})(\text{PMe}_3)_2]$ or a similar type of structure. Such a pathway might have been envisioned, for example, as stemming from changing the order of the M–N bond from three to two (as a result of dissociation of the nitrogen lone pair) followed by the coordination of the $\delta^-\text{H}-\delta^+\text{Si}$ polarized bond to the freed coordination site. However, all attempts to determine such a structure, either as intermediate or transition state, failed.

The question of how the intermediate **18** transforms into the kinetic product **19** is of interest. Given the agostic nature of **18**, a conceivable pathway might include phosphine dissociation and hydride migration from silicon to niobium to give the unsaturated species **23** (Figure 5). Silyl migration from nitrogen to the metal would then complete

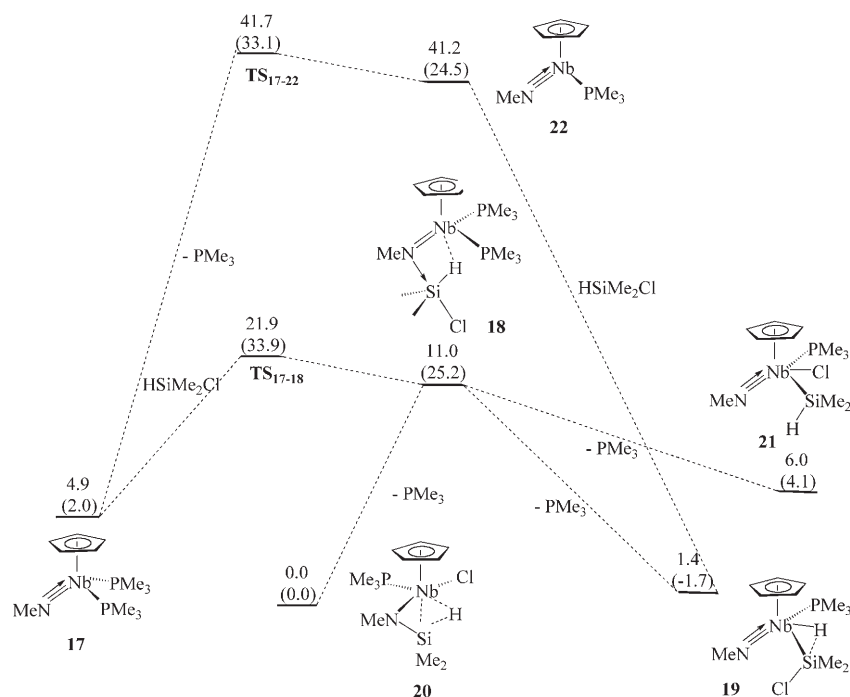


Figure 4. Relative electronic energies [kcal mol^{-1}] of intermediates and products in the reaction of $[\text{Nb}(\text{Cp})(=\text{NMe})(\text{PMe}_3)_2]$ with HSiMe_2Cl . Gibbs energies are given in brackets.

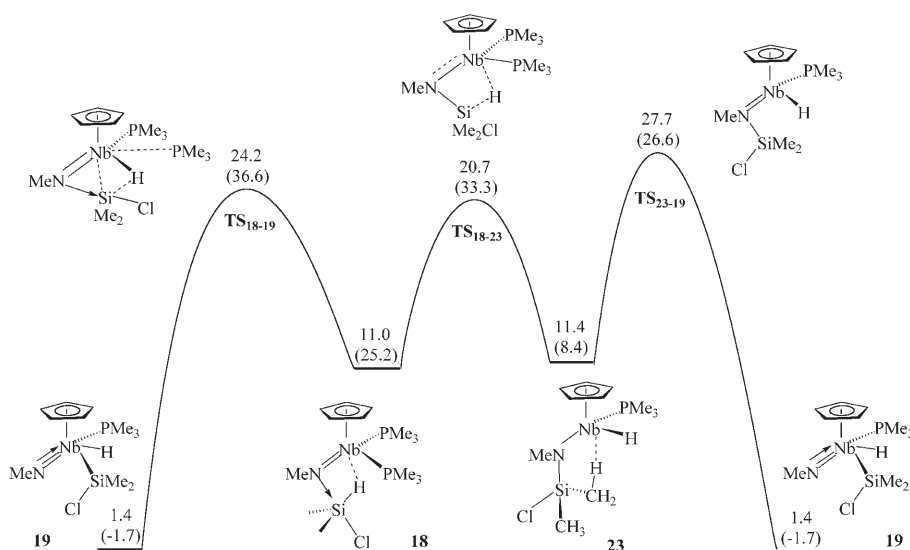


Figure 5. Two possible routes for the transformation of **18** into **19**. Relative electronic energies [kcal mol^{-1}]. Gibbs energies are given in parentheses.

this rearrangement. To determine the possible structure of **23**, we started from an anticipated geometry, in which the chlorine group on silicon was in the vicinity of metal, thus amenable to the donation of a chlorine lone pair to a vacant orbital on niobium to compensate for its unsaturation.^[40] To our surprise, the optimization revealed a structure with a significant separation (4.820 \AA) of the chloride group and the metal. In fact, there is a weak agostic bonding between

the methyl group on nitrogen and niobium ($\text{Nb}\cdots\text{H}$ distance of 2.404 \AA ; C-N-Nb bond angle of 99.7° versus a Si-N-Nb bond angle of 139.4°) instead of $\text{Cl}\rightarrow\text{Nb}$ donation. In spite of their pronounced structural differences, **23** was found to be only $0.4 \text{ kcal mol}^{-1}$ above **18**. However, it is much more stabilized on the Gibbs energy scale, owing to the favourable entropy change upon elimination of an equivalent of PMe_3 ($\Delta\Delta G = 16.8 \text{ kcal mol}^{-1}$). Transformation of **23** to **19** goes via a transition state TS_{23-19} , in which the silyl group is a slightly shorter distance from the metal than in **23**, and requires a modest activation barrier of $18.2 \text{ kcal mol}^{-1}$. Since TS_{23-19} lies only $1.4 \text{ kcal mol}^{-1}$ above the starting complex **18**, the highest barrier in the dissociative pathway is that separating **18** and **23** ($\Delta G^\ddagger = 8.1 \text{ kcal mol}^{-1}$).

We also found a transition state TS_{18-19} for the direct transformation of **18** into **19** (Figure 5). This pathway goes through a concerted silyl and hydride migration to niobium and requires a slightly higher barrier of $11.4 \text{ kcal mol}^{-1}$ (Gibbs energy scale). The relative stability of TS_{23-19} and TS_{18-19} is reversed on the electronic energy scale ($\Delta E = -3.5 \text{ kcal mol}^{-1}$). Thus, overall, a stepwise migration of hydride and silyl ligands from the imido group to niobium appears to be entropically favoured. However, the difference between TS_{18-23} and TS_{18-19} is close to the accuracy of our calculations, which does not allow us to make a clear-cut differentiation of the two mechanistic alternatives.

The reaction of **17** with the more acidic dichlorosilane HSiCl_2Me differs in that the direct addition of HSiMeCl_2 to the imido moiety to give the adduct **24** is by $0.9 \text{ kcal mol}^{-1}$ more stable on the electronic energy scale than the starting diphosphine complex (Figure 6). Although its formation is still thermodynamically disfavoured ($\Delta G_f = 16.1 \text{ kcal mol}^{-1}$) for entropic reasons, the dissociative pathway via the unsat-

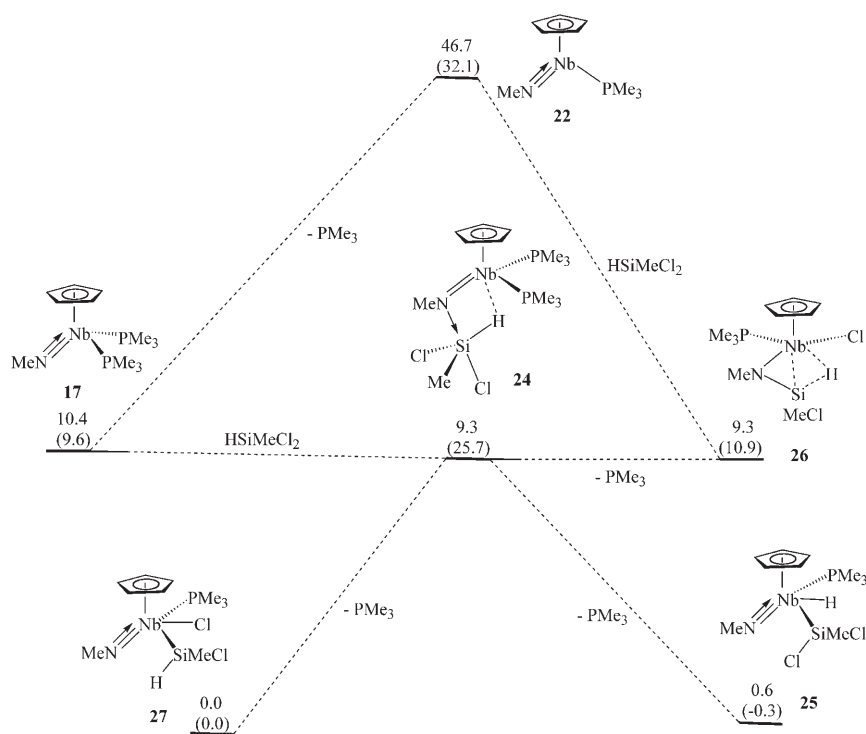


Figure 6. Relative electronic energies [kcal mol^{-1}] of stable intermediates and products in the reaction of $[\text{Nb}(\text{Cp})(=\text{NMe})(\text{PMe}_3)_2]$ with $\text{HSiMe}_2\text{Cl}_2$. Gibbs energies are given in brackets.

turated complex **22** turns out to be less profitable on both the electronic ($\Delta\Delta E = 37.4 \text{ kcal mol}^{-1}$) and Gibbs free energy scales ($\Delta\Delta G_f = 6.4 \text{ kcal mol}^{-1}$). Transformation of the silane adduct **24** into the agostic product **26** is thermodynamically feasible (Figure 6), but is by about 10 kcal mol^{-1} less favourable than the formation of silylhydride **25**. This accounts for our failure to observe this agostic species. In accord with our experimental findings, the “rearranged” chloride-silyl derivative **27** is the most stable product on the electronic energy scale, but is slightly disfavoured relative to **25** on the Gibbs energy scale. Again, these small differences are within the error margin of our calculations.

To summarize, DFT calculations of model complexes establish that an associative mechanism of silane addition to $[\text{Cp}(\text{RN}=\text{N})\text{Nb}(\text{PMe}_3)_2]$ is thermodynamically comparable with the dissociative mechanism in the case of HSiClMe_2 and is the preferred mechanism in the case of more acidic silane HSiCl_2Me .

DFT calculations—Structural aspects:

Silane/imido adducts: The structures of the calculated complexes are of interest too and deserve a more in depth discussion. As mentioned above, in addition to the anticipated penta-coordinate silicon centre the silane/imido adducts **18** and **24** display $\beta\text{-Si-H}\cdots\text{M}$ agostic bonding. For instance, in the compound **18** the Nb–H distance of 1.943 \AA is even shorter than the Nb–H distance in the β -agostic silylamido complex **20** (2.052 \AA). In the adduct of HSiMe_2Cl (**18**), the

unique chlorine atom lies *trans* to the nitrogen centre, whereas two methyl groups and the hydride form an equatorial plane of a distorted trigonal bipyramid. The apical Si–Cl bond is significantly elongated (2.446 \AA versus average 2.02 \AA in monochloro organosilanes),^[41] as is usually observed in hypervalent silicon compounds. The equatorial Si–H bond of 1.607 \AA in **18** is also much longer than the usual Si–H bond of 1.48 \AA , which can be attributed to the presence of agostic interaction. In the dichlorosilane adduct **24**, the apical Si–Cl bond is noticeably longer than the equatorial one (2.289 \AA versus 2.152 \AA), as expected. Surprisingly, the different substitution at silicon in the adducts **18** and **24** does not significantly affect the degree of Si–H bond activation in these compounds. For example, the Si–H bond of 1.607 \AA in **18** is identical within error to

1.609 \AA in **24**, and the Nb–H distances are also comparable (1.943 \AA versus 1.928 \AA , respectively). A similar situation, contradicting the common anticipation that more electron-withdrawing substituents at silicon lead to more advanced Si–H bond activation,^[42] has been very recently discovered in the related agostic complexes of molybdenum $[\text{Mo}(=\text{NR})\{\eta^3\text{-N}(\text{R})\text{SiMeX-H}\cdots\}(\text{Cl})(\text{PMe}_3)_2]$ ($\text{X} = \text{Me}$ or Cl).^[20] Such a behaviour can be rationalized in terms of near cancellation of the increased back-donation from metal to the $\sigma^*(\text{Si-H})$ antibonding orbital by the decreased direct donation from the $\sigma(\text{Si-H})$ bonding orbital to a vacant orbital on metal.^[20]

Silane coordination to the imido centre of the formally d^2 complex **17** results in the elongation of the Nb–N multiple bond. Thus, the Nb=N bond of 1.824 \AA in **17** elongates to 1.943 \AA in **18** upon the addition of HSiMe_2Cl . On the other hand, in the d^0 complexes **19**, **21**, **25** and **27**, the Nb–N bond is noticeably shorter (range $1.784\text{--}1.793 \text{ \AA}$). This is consistent with an incomplete electron lone pair transfer from the imido ligand to the metal in **17**, so that the character of the metal–imido bond should be regarded as intermediate between double and triple. Obviously, it is the electron deficiency of the metal centre, enhanced by the Lewis acid coordination to the imido group, which allows for the formation of the $\text{Si-H}\cdots\text{M}$ agostic bonding in the compounds **18** and **24**.

Mountford et al. have recently showed that in arylimido complexes $[\text{Ti}(\text{COT})(=\text{NR})]$ ($\text{COT} = \text{cyclooctatetraene}$) for $\text{R} = \text{Aryl}$ the electron density of the ring is effectively delocalized on the $\text{M}=\text{N}$ linkage, pushing the nitrogen lone pair

higher in energy and thus making it more amenable for an attack of an electrophile.^[43] On the other hand, Sundermeyer et al. considered the multiple metal-nitrogen bond in half-sandwich silylimido complexes to be in the limit of π -saturation (i.e. a genuine triple $M\equiv N$ bond).^[44] These arguments and the findings of the current work allows us to rationalize the earlier observed discrepancy in the reactivity of the compounds $[\text{Nb}(\text{Cp})(=\text{NAr})(\text{PMe}_3)_2]$ and $[\text{Nb}(\text{Cp})(=\text{N}t\text{Bu})(\text{PMe}_3)_2]$.^[18] It is the lack of electron density on the nitrogen centre in the latter that prevents the effective coupling of silane with the imido moiety.

Silyl hydrido complexes: The calculated structures of the silyl hydrido complexes **19** and **25** are consistent with the presence of IHI.^[14–16, 18, 28] There is a very good agreement with the previously calculated tantalum complexes $[\text{Ta}(\text{Cp})(=\text{NMe})(\text{PMe}_3)(\text{H})(\text{SiMe}_n\text{Cl}_{3-n})]$ ($n=0–3$).^[28] In particular, the Si–H contacts are shortened^[14–16, 18, 28] (2.035 and 2.052 Å, respectively) and two types of Si–Cl bonds^[15, 28] (one elongated (2.144 Å), *trans* to hydride, and one normal (2.124 Å)) were observed in **25**. IHI consists of electron density transfer from electron-rich metal-hydride bond on the antibonding $\sigma^*(\text{Si}-\text{X})$ orbital of the *trans* Si–X bond, leading to the elongation of M–H bond, the contraction of M–Si bond and the elongation of Si–X bond.^[14–16, 18, 28] Obviously, the overlap of $\sigma(\text{M}-\text{H})$ and $\sigma^*(\text{Si}-\text{X})$ is optimal when substituent X at Si is *trans* to hydride.^[14]

To verify this stereochemical aspect of IHI, we also calculated a “*cis*-rotamer” of **19** in which the position *trans* to the hydride is occupied by the methyl group. The complex **19-cis**, although having almost identical steric properties as **19**, is destabilized by 2–3 kcal mol⁻¹, owing to the loss of IHI. The rotation of silyl group leads to a shorter Nb–H bond (1.793 Å in **19-cis** versus 1.811 Å in **19**), longer Nb–Si bond (2.587 Å in **19-cis** versus 2.576 Å in **19**), shorter Si–Cl bond (2.149 Å in **19-cis** versus 2.171 Å in **19**) and longer Si–H distances (2.075 Å in **19-cis** versus 2.035 Å in **19**). The short Nb–H bond of 1.793 Å in **19** compares well with the classical Nb–H bond of 1.765 Å in **23**, further substantiating our conclusion that IHI causes relative elongation of the M–H bonds.^[14–18, 22] These minor differences in energy and bond lengths are of little importance when ground states only are considered, but can be vital in differentiating between transition states or reactive intermediates in metal mediated transformations of organosilanes.

Interestingly, optimization of another isomer of **19**, which has the silyl ligand *cis* to the PMe_3 group, converged to a σ -complex type structure $[\text{Nb}(\text{Cp})(=\text{NAr})(\text{PMe}_3)(\eta^2\text{-H}-\text{SiMe}_2\text{Cl})]$ that has a Si–H distance of 2.012 Å and an elongated Nb–Si distance of 2.697 Å (2.576 Å in **19**). In contrast, the Nb–H distance of 1.741 Å is normal for a Nb–Hydride bond and is comparable with the one in **23**. These data are compatible with the presence of a stretched silane σ -complex, which is formed to minimize the steric repulsion between bulky PMe_3 and SiMe_2Cl groups.^[21e] This view is supported by significant elongation of the Nb–P distance of 2.668 Å versus 2.542 Å in **19**.

Agostic complexes: The structure of agostic complex **20** is in good accord with our previous calculation employing the BP86 potential.^[18] The agostic species **26**, featuring a chloride group on the silicon centre, has a less activated Si–H bond (i.e. stronger Si–H interaction) than its dimethyl substituted analogue **20**. For example, the Nb–H bond elongates (2.052 Å in **20** versus 2.218 Å in **26**) whereas the Si–H bond contracts (1.556 Å in **20** versus 1.507 Å in **26**). Weaker Nb–H interaction in **26** corresponds well to longer Nb–Si distance (2.792 Å). Such a weakening of agostic Si–H \cdots M bonding upon chlorine-for-methyl substitution contradicts the usual observation that electron-accepting groups at silicon promote stronger Si–H bond activation^[42] and can be rationalized in terms of decreased basicity of the Si–H bond caused by the presence of an electron-withdrawing chlorine group at silicon.^[20]

Conclusion

The imido ligand has been intensively studied as an isolobal analogue of the ubiquitous Cp ligand, and in particular has been extensively used in designing new olefin metathesis and polymerization catalysts and silane σ -bond metathesis catalysts. This work presents a study case when the imido ligand shows a distinctly non-innocent behaviour toward silanes: it either transforms itself into an agostic silylamido ligand or acts as a “chemical smuggler” in silane transfer to the metal when the final products appear to have an intact imido ligand, such as in complexes $[\text{Nb}(\text{Cp})(=\text{NR}')(\text{PMe}_3)(\text{H})(\text{SiR}_n\text{Cl}_{3-n})]$, $[\text{Nb}(\text{Cp})(=\text{NR}')(\text{PMe}_3)(\text{Cl})(\text{SiHR}_n\text{Cl}_{2-n})]$ or $[\text{Nb}(\text{Cp})(=\text{NR}')(\text{PMe}_3)\text{Cl}_2]$. Combined experimental and theoretical evidence tends to suggest that direct silane addition to imido group is a realistic mechanistic concurrent with a “text-book” pathway based on phosphine dissociation from the 18e precursor $[\text{Nb}(\text{Cp})(=\text{NR}')(\text{PMe}_3)_2]$ and Si–H addition to the 16e intermediate $[\text{Nb}(\text{Cp})(=\text{NR}')(\text{PMe}_3)]$. According to the new mechanism, reactions of complexes $[\text{Nb}(\text{Cp})(=\text{NR}')(\text{PR}'_3)_2]$ with silanes proceeds via an intermediate adduct $[\text{Nb}(\text{Cp})\{\text{N}(\rightarrow\text{SiHClR}_2)\text{R}'\}(\text{PR}'_3)_2]$ that rearranges into the initial products $[\text{Nb}(\text{Cp})(=\text{NR}')(\text{PR}'_3)(\text{H})(\text{SiR}_3)]$ and/or $[\text{Nb}(\text{Cp})\{\eta^3\text{-N}(\text{R}')\text{SiR}_2\text{Cl}-\text{H}\cdots\}(\text{PR}'_3)(\text{Cl})]$. Conversion of kinetic products into the thermodynamic products is catalyzed by phosphine addition and proceeds via the same intermediate $[\text{Nb}(\text{Cp})\{\text{N}(\rightarrow\text{SiHClR}_2)\text{R}'\}(\text{PR}'_3)_2]$. The identity of these products is controlled by the substitution at silicon and nitrogen and the steric properties of the phosphine. Donor groups at silicon in chlorosilanes and smaller substituents at nitrogen favour the formation of β -Si–H \cdots Nb agostic products, whereas electron-withdrawing groups at silicon stabilize metal silyl derivatives. The lower stability of agostic product in the case of HSiCl_2Me addition in comparison with HSiClMe_2 can be ascribed to the lower basicity of the Si–H bond caused by the presence of an accepting chlorine group at silicon in the former.

The initial products of silane addition to $[\text{Nb}(\text{Cp})(=\text{NR}')(\text{PR}_3)_2]$ are metastable if there are two or three chlorine groups at silicon atom, decomposing in the presence of phosphine to complexes $[\text{Nb}(\text{Cp})(=\text{NAr})(\text{PMe}_3)(\text{Cl}) (\text{SiHR}_n\text{Cl}_{2-n})]$, $[\text{Nb}(\text{Cp})(=\text{NAr})(\text{PMe}_3)_2\text{Cl}_2]$, and/or to $[\text{Nb}(\text{Cp})(\text{PMe}_3)_3\text{Cl}_2]$. These findings suggest that imido-group may be not a good platform for supporting σ -bond metathesis type reactions because of its possible involvement in the activation of E–X bonds. This conclusion can have far-reaching implications for the current research in the field of early-transition metal catalysis of silane transformations.^[45,50]

Experimental Section

All manipulations were carried out using conventional glove-box and Schlenk techniques. Solvents were dried over sodium or sodium benzophenone ketyl. NMR spectra were recorded on a Varian Mercury-vx (¹H, 300 MHz; ¹³C, 75.4 MHz; ³¹P, 121.5 MHz) and Unity-plus (¹H, 500 MHz; ¹³C, 125.7 MHz) spectrometers. IR spectra were obtained as Nujol mulls with a FTIR Perkin–Elmer 1600 series spectrometer. Silanes were obtained from Sigma–Aldrich and Lancaster and distilled over CaH₂. Starting complexes $[\text{Nb}(\text{Cp})(=\text{NR}')(\text{Cl})_2]$ and $[\text{Nb}(\text{Cp})(=\text{NR}')(\text{PR}'_3)_2]$ (R' = Ar, Ar'; R'₃P = Me₃P, PhMe₂P) were prepared in analogy with literature methods (see Supporting information for details). Compounds **2b** and **7b** were previously reported.^[18]

[Nb(Cp)(=NAr)(PMe₃)(H)(SiMePhH)] (3a): H₂SiMePh (0.52 mL, 3.80 mmol) was added through a syringe to a toluene solution (15 mL) of $[\text{Nb}(\text{Cp})(=\text{NAr})(\text{PMe}_3)_2]$ (0.37 g, 0.76 mmol). The mixture was left for two days under stirring and constant purging with nitrogen. The volatiles were removed in vacuo, affording yellow-brown oil. NMR spectra showed quantitative formation of $[\text{Nb}(\text{Cp})(=\text{NAr})(\text{PMe}_3)(\text{H})(\text{SiMePhH})]$ as a mixture of two isomers. IR (Nujol): $\tilde{\nu}$ = 2068 (Si–H), 1644 cm⁻¹ (Nb–H).

First isomer: ¹H NMR (C₆D₆): δ = 7.96 (d, $J(\text{H–H})$ = 8.0 Hz, 2H; Ph), 7.33–6.95 (m, 6H; C₆H₃ + Ph), 5.96 (h, $J(\text{H–H})$ = 3.7 Hz, 1H; Si–H), 5.27 (d, $J(\text{P–H})$ = 1.8 Hz, 5H; Cp), 4.11 (q, $J(\text{H–H})$ = 6.9 Hz, 2H; CHMe₂), 2.02 (d, $J(\text{P–H})$ = 67 Hz, 3H; Nb–H), 1.28 (d, $J(\text{H–H})$ = 6.9 Hz, 6H; CHMe₂), 1.23 (d, $J(\text{H–H})$ = 6.9 Hz, 6H; CHMe₂), 0.95 (dd, $J(\text{H–H})$ = 4.1 Hz, $J(\text{P–H})$ = 0.7 Hz, 3H; SiMe), 0.90 ppm (d, $J(\text{P–H})$ = 8.4 Hz, 9H; PMe₃).

Second isomer: ¹H NMR (C₆D₆): δ = 7.88 (d, $J(\text{H–H})$ = 8.0 Hz, 2H; Ph), 5.96 (q, $J(\text{H–H})$ = 3.7 Hz, 1H; Si–H), 5.29 (d, $J(\text{P–H})$ = 1.8 Hz, 5H; Cp), 4.06 (h, $J(\text{H–H})$ = 6.8 Hz, 2H; CHMe₂), 1.27 (d, $J(\text{H–H})$ = 6.9 Hz, 6H; CHMe₂), 1.17 (d, $J(\text{H–H})$ = 6.9 Hz, 6H; CHMe₂), 0.98 (d, $J(\text{H–H})$ = 4.0 Hz, 3H; SiMe), 0.91 (d, $J(\text{P–H})$ = 8.1 Hz, 9H; PMe₃), 2.24 ppm (d, $J(\text{P–H})$ = 68 Hz, 3H; Nb–H); ³¹P NMR (C₆D₆): δ = 14.0 ppm (b); ²⁹Si NMR (C₆D₆): δ = 13.3 ppm (¹J(Si–H) = 156 Hz, ²J(Si–H) < 15 Hz (estimated from the line width)).

Isolation of [Nb(Cp)(=NAr)(PMe₃)(H)(SiMe₂Cl)] (3b): To $[\text{Nb}(\text{Cp})(\text{NAr})\text{NbPMe}_3)_2]$ (0.202 g, 0.42 mmol) in pentane (20 mL) was added excess HClSiMe₂ (1.5 mL). After 1.5 h of stirring at room temperature the initial dark solution developed a distinctly green-yellow colour. The solution was concentrated in vacuo to 3 mL and filtered off, the residue was washed by 1.5 mL of pentane and dried in vacuo. Yield: 0.018 g (0.04 mmol, 9%). ¹H NMR (C₆D₆): δ = 5.56 (d, $J(\text{P–H})$ = 1.5 Hz, 5H; Cp), 4.14 (sept, $J(\text{P–H})$ = 6.9 Hz, 2H; CH), 1.65 (broad s, 1H; NbH), 1.26 (d, $J(\text{H–H})$ = 7.2 Hz, 6H; Me), 1.24 (d, $J(\text{H–H})$ = 7.2 Hz, 6H; Me), 1.19 (s, 3H; SiMe), 0.92 (s, 3H; SiMe), 0.83 ppm (d, $J(\text{P–H})$ = 8.1 Hz, 9H; PMe₃); ¹³C NMR (C₆D₆): δ = 143.4, 123.3, 122.8 (C₆H₃), 100.9 (Cp), 27.1 (CH), 24.4, 24.3, 19.5 (d, $J(\text{C–P})$ = 26.9 Hz, PMe₃), 14.9 (Si–Me), 14.4 ppm (Si–Me); IR (Nujol): $\tilde{\nu}$ = 1681 cm⁻¹ (Nb–H). Analogous Ta compound was prepared and fully characterized.^[18]

Reaction of [Nb(Cp)(=NAr)(PMe₃)₂] with HSiMePhCl: To a pentane solution (40 mL) of $[\text{Nb}(\text{Cp})(=\text{NAr})(\text{PMe}_3)_2]$ (0.522 g, 1.08 mmol) was added HSiMePhCl (0.16 mL, 1.08 mL). The mixture was left at room temperature in dark for 3 days. The solution was filtered from small amount of grey deposit and left at –30 °C for 5 days, affording a grey precipitate. After keeping the mixture at –80 °C for a day the cold solution was filtered, the residue dissolved in ether, filtered and cooled to –80 °C, affording a light-beige microcrystalline compound. The yield: 0.18 g (0.32 mmol, 30%). The second crop was obtained by concentrating the mother liquor to 4 mL and cooling it to –80 °C. Total yield: 0.28 g (0.50 mmol, 46%); IR (Nujol): $\tilde{\nu}$ = 1632 cm⁻¹ (Nb–H, broad, overlapping signals due to **2c** and **3c**); elemental analysis calcd (%) for C₂₇H₄₀ClNNbPSi: C 57.29, H 7.12, N 2.47; found: C 56.52, H 6.15, N 2.13. The ¹H NMR showed formation of a mixture of two isomers of agostic complex and two isomers (Ph up and Ph down) of a silylhydride complex:

Agostic major (2c): ¹H NMR (C₆D₆): δ = 7.48 (m, Ph), 4.73 (d, $J(\text{P–H})$ = 1.7 Hz, 5H; Cp), 2.83 (q, $J(\text{H–H})$ = 6.9 Hz, 1H; CHMe₂), 2.57 (q, $J(\text{H–H})$ = 6.9 Hz, 1H; CHMe₂), 1.11 (d, $J(\text{H–H})$ = 6.9 Hz, 1H; CHMe₂), 1.11 (d, $J(\text{H–H})$ = 6.9 Hz, 1H; CHMe₂), 0.98 (d, $J(\text{P–H})$ = 10.2 Hz, 9H; PMe₃), 0.59 (s, 3H; SiMe), –4.75 ppm (d, J = 9.1 Hz, 1H; Nb–H); ¹³C NMR (C₆D₆): δ = 93.8 (s, Cp), 17.9 ppm (d, $J(\text{P–C})$ = 24 Hz, PMe₃); ³¹P NMR (C₆D₆): δ = 9.5 ppm.

Agostic minor (2c'): ¹H NMR (C₆D₆): δ = 4.83 (d, $J(\text{P–H})$ = 1.7 Hz, 5H; Cp), –3.23 ppm (s, 1H; Nb–H); ¹³C NMR (C₆D₆): δ = 95.6 ppm (s, Cp).

Silylhydride major (3e): ¹H NMR (C₆D₆): δ = 8.06 (d, $J(\text{H–H})$ = 8.5 Hz, 2H; Ph), 7.31 (pseudo t, $J(\text{H–H})$ = 7.3 Hz, 2H; Ph), 7.17 (m, Ph), 7.05 (m, Ph), 5.40 (d, J = 1.6 Hz, 5H; Cp), 2.15 (d, $J(\text{P–H})$ = 64.1 Hz, 1H; Nb–H), 4.16 (q, $J(\text{H–H})$ = 6.9 Hz, 1H; CHMe₂), 1.27 (d, $J(\text{H–H})$ = 6.9 Hz, 1H; CHMe₂), 1.23 (d, $J(\text{H–H})$ = 6.9 Hz, 1H; CHMe₂), 0.93 ppm (d, $J(\text{P–H})$ = 8.1 Hz, 9H; PMe₃); ¹³C NMR (C₆D₆): δ = 101.6 (s, Cp), 24.5 (s, CHMe₂), 23.3 (s, CHMe₂), 19.5 (d, $J(\text{P–C})$ = 28 Hz, PMe₃), 13.8 ppm (s, SiMe); ³¹P NMR (C₆D₆): δ = 12.5 ppm.

Silylhydride minor (3e''): ¹H NMR (C₆D₆): δ = 8.20 (d, $J(\text{H–H})$ = 8.5 Hz, 2H; Ph), 5.61 (d, J = 1.6 Hz, 5H; Cp), 3.95 (q, $J(\text{H–H})$ = 6.9 Hz, 1H; CHMe₂), 2.19 (d, $J(\text{P–H})$ = 64.1 Hz, 1H; Nb–H), 1.37 (d, $J(\text{H–H})$ = 6.9 Hz, 1H; CHMe₂), 1.15 ppm (d, $J(\text{H–H})$ = 6.9 Hz, 1H; CHMe₂); ¹³C NMR (C₆D₆): δ = 101.4 (s, Cp), 19.4 (d, $J(\text{P–C})$ = 28 Hz, PMe₃); ³¹P NMR (C₆D₆): δ = –11.7 ppm.

Complexes 2c, 2c' and 3c: ²⁹Si NMR (C₆D₆): δ = –51 ppm (¹J(Si–H) = 96 Hz, “agostic”, Cl *trans* to H), –72 (¹J(Si–H) = 121 Hz, “agostic”, PMe₃ *trans* to H), 78.8 ppm (broad, “silylhydride”).

[Nb(Cp)(=NAr)(PMe₃)(H)(SiMeCl₂)] (3d): HSiMeCl₂ (0.15 mL, 1.44 mmol) was added to a cooled (–30 °C) pentane solution (40 mL) of **1** (0.40 g, 0.82 mmol). The cold mixture was kept at –30 °C overnight. Dark yellow crystals formed. The mother liquor was filtered and the residue dried in vacuo. Yield: 0.287 g (0.55 mmol, 67%). ¹H NMR (C₆D₆): δ = 5.46 (d, $J(\text{P–H})$ = 1.8 Hz, 5H; Cp), 3.97 (h, $J(\text{H–H})$ = 6.8 Hz, 2H; CHMe₂), 2.51 (d, $J(\text{P–H})$ = 70.2 Hz, 1H; Nb–H), 1.48 (s, 3H; Si–Me), 1.21 (d, $J(\text{H–H})$ = 6.8 Hz, 6H; CHMe₂), 1.17 (d, $J(\text{H–H})$ = 6.8 Hz, 6H; CHMe₂), 0.83 ppm (d, $J(\text{P–H})$ = 8.5 Hz, 1H; P–Me); ¹³C NMR (C₆D₆): δ = 143.5, 124.0, 122.8, 102.4 (Cp), 27.3, 24.3, 24.2, 19.2 ppm (d, $J(\text{P–C})$ = 28.3 Hz, P–Me); ³¹P NMR (C₆D₆): δ = 11.4 ppm (b); IR (Nujol): $\tilde{\nu}$ = 1620 cm⁻¹ (Nb–H); elemental analysis calcd (%) for C₂₁H₃₅Cl₂NNbPSi: C 48.10, H 6.73, N 2.67; found: C 48.08, H 7.26, N 2.52.

[Nb(Cp)(=NAr)(PMe₃)(H)(SiCl₃)] (3e): HSiCl₃ (0.12 mL, 1.12 mmol) was added through a syringe to a solution of **1** (0.270 g, 0.56 mmol) in ether (10 mL) resulting in a quick colour change to yellow. All volatiles were removed at reduced pressure and the residue was redissolved in 15 mL of ether, filtered, concentrated to 10 mL and charged with 1 mL of pentane. The mixture was placed in the –30 °C freezer for a day, affording yellow crystals (0.035 g). The cold solution was decanted and placed in –80 °C for 2 days, resulting in further crystallization. Combined yield: 0.237 g (78%). ¹H NMR (C₆D₆): δ = 7.00 (d, $J(\text{H–H})$ = 3.6 Hz, 1H; Ar), 6.98 (s, 2H; *m*-Ar), 6.92 (m, 1H; *p*-Ar), 5.58 (d, $J(\text{P–H})$ = 1.5 Hz, 5H; Cp), 3.96 (h, $J(\text{H–H})$ = 6.9 Hz, 2H; CHMe₂), 3.00 (d, $J(\text{P–H})$ = 72.6 Hz, 1H; NbH), 1.25 (d, $J(\text{H–H})$ = 6.9 Hz, 6H; CHMe₂), 1.17 (d, $J(\text{H–H})$ =

(C₆D₆): δ = 10.8 ppm (bs); ¹³N NMR (C₆D₆): δ = 102.0 (Cp), 23.0 (Ar'), 19.0 ppm (PMe₃); ³¹P NMR (C₆D₆): 2 ppm (bs); IR (Nujol): ν = 1632 cm⁻¹ (Nb–H). Signals attributed to [Nb(Cp){ η^3 -N(Ar)SiPh₂-H \cdots }(PMe₃)(Cl) (**7f**): ¹H NMR (C₆D₆): δ = 4.79 (s, 5H; Cp), 2.10 (s, 6H; C₆H₃Me₂), 0.67 (bd, *J*(P–H) = 3.9 Hz, 9H; PMe₃), –2.05 ppm (bs, 1H; Nb–H), other signals are obscured by the signals of other products.

NMR tube preparation of [Nb(Cp)(=NAr)(SiMeCl₂)(H)(PPhMe₂)] (11d**):** Two equivalents of the silane HSiMeCl₂ were added to [Nb(Cp)(=NAr)(PPhMe₂)₂] (0.019 g) in C₆D₆ (0.6 mL). The spectrum run after 29 min showed 10% conversion into **11d**. After 24 h the reaction was complete, with **11d** being the predominant component of the mixture. After 13 days a 1:1 mixture of **11d** and [Nb(Cp)(=NAr)(SiMeClH)(Cl)(PPhMe₂)] was discovered [Nb(Cp)(=NAr)(SiMeCl₂)(H)(PPhMe₂)]. ¹H NMR (C₆D₆): δ = 7.41 (m, Ar/Ph), 7.30 (m, Ar/Ph), 7.01–7.00 (m, Ar/Ph), 5.63 (s, 5H; Cp), 3.29 (sept, *J*(H–H) = 6.8 Hz, 2H; 2 × CHMe₂), 2.72 (d, *J*(P–H) = 66.3 Hz, 1H; Nb–H), 1.47 (s, 3H; SiMe), 1.25 (d, *J*(P–H) = 17.7 Hz, 9H; PMe), 1.15 (d, *J*(H–H) = 6.6 Hz, 6H; *p*-CHMe₂), 1.13 ppm (d, *J*(H–H) = 7.5 Hz, 6H; CHMe₂); ³¹P NMR (C₆D₆): δ = 20 ppm (very broad); IR (Nujol): $\tilde{\nu}$ = 1621 cm⁻¹ (Nb–H).

[Nb(Cp){ η^3 -N(Ar)SiMe₂-H \cdots }]NbCl(PPhMe₂) (12b**):** HSiMe₂Cl (0.25 mL, 2.3 mmol) was added to a stirred suspension of [Nb(Cp)(=NAr)(PPhMe₂)₂] (0.491 g, 0.81 mmol) in hexane (15 mL). The mixture obtained was placed in the dark for a week, affording a dark precipitate. The mixture was cooled –20 °C, the supernatant solution was decanted and the residue was washed several times by hexanes (total volume 10 mL). The product was recrystallized from ether by cooling the solution to –20 °C. The yield of dark green crystals: 0.050 g (11%). ¹H NMR (C₆D₆): δ = 7.34 (t, *J*(H–H) = 8.8 Hz, 2H; *m*-Ph), 7.26 (d, *J*(H–H) = 7.2 Hz, 1H; *m*-Ar), 7.19 (d, *J*(H–H) = 7.2 Hz, 1H; *m*-Ar), 7.04 (m, 3H; *o*-Ph and *p*-Ar), 4.63 (d, *J*(P–H) = 2.1 Hz, 5H; C₅H₅), 3.30 and 2.35 (sept, *J*(H–H) = 7.0 Hz, 2H; 2 × CHMe₂), 1.49 (d, *J*(H–H) = 6.9 Hz, 6H; 3 × CHMe₂), 1.42 (d, *J*(H–H) = 6.9 Hz, 3H; PMe₂), 1.37 (d, *J*(H–H) = 6.9 Hz, 3H; PMe₂), 1.32 (d, *J*(H–H) = 6.9 Hz, 3H; 2 × CHMe₂), 1.28 (d, *J*(H–H) = 6.9 Hz, 3H; 2 × CHMe₂), 1.12 (d, *J*(H–H) = 6.9 Hz, 3H; 2 × CHMe₂) 0.36 (s, 3H; SiMe₂H), 0.19 (s, 3H; SiMe₂H), –5.63 ppm (bs, 1H; Nb–H); ¹³N NMR (C₆D₆): δ = 149.0 (*i*-Ar), 141.1 (*o*-Ar), 139.4 (*o*-Ar), 130.3 (d, *J*(P–C) = 9.0 Hz, *m*-Ph), 129.2 (Ph), 128.5 (*o*-Ph), 123.5 (*p*-Ar), 123.2 (*m*-Ar), 123.4 (*m*-Ar), 94.6 (Cp), 27.7 (CHMe₂), 27.4 (CHMe₂), 26.9 (CHMe₂), 25.7 (CHMe₂), 25.2 (CHMe₂), 24.5 (CHMe₂), 17.9 (d, *J*(P–C) = 21.5 Hz, PMe), 14.2 (d, *J*(P–C) = 22.8 Hz, PMe), 3.5 (SiMe), 1.9 ppm (SiMe); ³¹P NMR: δ = 33.5 ppm (bs); ²⁹Si NMR: δ = –52.9 ppm (d, *J*(H–Si) = 100.0 Hz); IR (Nujol): $\tilde{\nu}$ = 1617 cm⁻¹ (Si–H); elemental analysis calcd (%) for C₂₇H₄₀ClNbNPSi: C 57.29, H 7.12, N 2.47; found: C 57.31, H 7.27, N 2.20.

[Nb(Cp)(=NAr)(SiMeHCl)(Cl)(PPhMe₂)] (13d**):** HSiMeCl₂ (0.2 mL, 2.0 mmol) was added to a solution of [Nb(Cp)(=NAr)(PPhMe₂)₂] (0.294 g, 0.48 mmol) in THF (10 mL). The mixture was left for 4 weeks in the dark at room temperature. This resulted in a yellow-brown solution over a small amount of yellow precipitate. The solution was concentrated to 2 mL and charged by pentane (4 mL), resulting in precipitation of a yellow-brown solid. The precipitate was filtered, washed by 1 mL of pentane and dried to give 0.034 g (0.06 mmol, 12%) of **13d**. ¹H NMR (C₆D₆): δ = 7.85 (d, *J*(H–H) = 6.6 Hz, 2H; *o*-Ph), 7.31 (t, *J*(H–H) = 7.2 Hz, 1H; *p*-Ph), 7.24 (t, *J*(H–H) = 6.6 Hz, 2H; *m*-Ph), 7.11 (d, *J*(H–H) = 8.1 Hz, 2H; *m*-Ar), 6.98 (pt, *J*(H–H) = 7.4 Hz, 1H; *p*-Ar), 6.17 (q, *J*(H–H) = 3.8 Hz, 1H; SiHClMe), 5.27 (d, *J*(P–H) = 1.5 Hz, 5H; Cp), 4.08 (sept, *J*(H–H) = 6.9 Hz, 2H; CHMe₂), 1.30 (d, *J*(H–H) = 7.5 Hz, 6H; CHMe₂), 1.24 (d, *J*(H–H) = 6.6 Hz, 6H; CHMe₂), 1.02 (d, *J*(H–H) = 4.5 Hz, 3H; SiMeHCl), 1.94 ppm (d, *J*(P–H) = 9.0 Hz, 6H; PPhMe₂); ¹³N NMR (C₆D₆): δ = 153.1 (s, *i*-Ph), 149.1 (s, *i*-Ar'), 143.1 (s, *o*-Ar'), 135.6 (s, *o*-Ph), 127.9 (s, *t*-Ph), 127.1 (s, *m*-Ph), 122.7 (s, *m*-Ar'), 122.5 (s, *p*-Ar'), 99.4 (s, Cp), 27.3 (s, CHMe₂), 24.4 (s, CHMe₂), 24.35 (s, CHMe₂), 19.9 ppm (d, *J*(P–C) = 29.7 Hz, PPhMe₂); ³¹P NMR: δ = –1.6 ppm (s); IR (Nujol): ν = 1622 cm⁻¹ (Nb–H); elemental analysis calcd (%) for C₂₆H₃₇Cl₂NbNPSi: C 53.25, H 6.36, N 2.38; found: C 49.22, H 5.87, N 1.80.

[Nb(Cp){ η^3 -N(Ar')SiMe₂-H \cdots }]Cl(PPhMe₂) (15b**):** Excess of HSiMe₂Cl (0.20 mL, 1.8 mmol) was added to a suspension of 0.315 g (0.57 mmol) of

[Nb(Cp)(=NAr')(PPhMe₂)₂] in hexane (10 mL). A grey-green precipitate started to form immediately upon the addition, accompanied by the colour change from dark-purple to dark-green. In 1 h the solution became lighter and dark-green needles deposited. Next day, the crystalline precipitate was washed with hexane and dried. The yield: 0.105 g (36%). ¹H NMR (C₆D₆): δ = 7.13 (d, obscured by C₆D₆, *o*-Ar), 7.06 (t, *J*(H–H) = 8.0, 1H; *p*-Ph), 7.0–6.88 (m, 5H; *m*-PPh and Ar'), 4.70 (d, *J*(P–H) = 1.5 Hz, 5H; C₅H₅), 2.96 (s, 3H; C₆H₃Me₂), 1.24 (d, *J*(P–H) = 7.5 Hz, 3H; PMe), 1.08 (s, 3H; C₆H₃Me₂), 1.03 (d, *J*(P–H) = 6.6 Hz, 3H; PMe₂), 0.53 (s, 3H; SiMe), –0.24 (bs, 3H; SiMe), –3.48 ppm (bs, 1H; Nb–H); ¹³N NMR (C₆D₆): δ = 130.1 (bs, *o*-Ar'), 129.6 (d, *J*(P–C) = 9.0 Hz, *o*-Ph), 129.4, 129.0, 128.7, 128.2, 122.8 (s, Ar'), 96.8 (s, C₅H₅), 20.5 (s, Me), 19.0 (s, Me), 13.5 (bs, PMe₂), 13.3 (bs, PMe₂), 0.1 (s, SiMe₂), –2.0 ppm (s, SiMe₂); ³¹P NMR: δ = 15.5 ppm (bs); ²⁹Si NMR: δ = –67.8 ppm (d, *J*_{H-Si} = 132 Hz); IR (Nujol): $\tilde{\nu}$ = 1622 cm⁻¹ (Nb–H); elemental analysis calcd (%) for C₂₁H₃₂ClNNbPSi: C 54.17, H 6.33, N 2.75; found: C 55.44, H 7.20, N 2.44.

[V(Cp)(=NAr)(PMe₃)(H)(SiMeCl₂)] (16**):** HSiMeCl₂ (0.20 mL, 1.92 mmol) was added to a pentane solution (20 mL) of [V(Cp)(=NAr)(PMe₃)₂] (0.50 g, 1.13 mmol). A dark-green solution was formed in 30 min at room temperature and crystallization of green needles began. The mixture was placed overnight in the –30 °C freezer. The mother liquor was filtered; the residue was washed by pentane (4 mL) and dried in vacuo. Yield: 0.112 g (0.23 mmol, 21%). Second crop (0.130 g, 0.24 mmol, 24%) was obtained by cooling the mixture to –30 °C. ¹H NMR (C₆D₆): δ = 6.94 (m, 2H; Ar), 6.88 (m, 2H; Ar), 5.28 (s, 5H; Cp), 4.17 (h, *J*(H–H) = 6.9 Hz, 2H; CHMe₂), 2.60 (d, *J*(P–H) = 48 Hz, 1H; V–H), 1.37 (s, 3H; Si–Me), 1.18 (d, *J*(H–H) = 6.9 Hz, 6H; CHMe₂), 1.17 (d, *J*(H–H) = 6.9 Hz, 6H; CHMe₂), 0.86 ppm (d, *J*(P–H) = 8.5 Hz, 1H; P–Me); ¹³C NMR (C₆D₆): δ = 94 ppm (s, Cp), other signals cannot be assigned due to decomposition during acquisition; IR (Nujol): $\tilde{\nu}$ = 1672 cm⁻¹ (V–H); elemental analysis calcd (%) for C₂₁H₃₅Cl₂NVPSi: C 52.28, H 7.31, N 2.90; found: C 51.90, H 7.76, N 2.73.

DFT calculations: All calculations were carried out with the Gaussian 03 program package^[46] using DFT applying the Becke three parameter hybrid exchange functional^[47a] in conjunction with the gradient-corrected non-local correlation functional of Perdew and Wang (B3PW91).^[47b] The compound basis set used for the calculation consisted of the 6-31G(d) basis set for the Si, P, N and Cl atoms, 6-31G for the carbon atoms and the 3-21G basis set for the H atoms of the Cp ring and Me groups. The basis set augmented by the p-polarization function (6-31G(d,p) basis set) was used for the hydride H atom. The Hay-Wadt effective core potentials (ECP) and the corresponding VDZ basis sets were used for the Nb atom.^[48]

X-ray structure analyses: The crystals of **3e**, **3g** and **15b** were grown from ethereal solutions by cooling to –30 °C. For all compounds, the crystals were mounted in a film of perfluoropolyether oil on a glass fibre and transferred to an Enraf–Nonius KappaCCD diffractometer. For all structures the data were corrected for Lorentz and polarization effects. The structures were solved by direct methods and refined by full-matrix least squares procedures.^[49] All non-hydrogen atoms were refined anisotropically. In the case of **3e** and **3g**, the hydride atoms were located from Fourier difference synthesis and positionally refined isotropically subject to a loose Nb–H distance restraint, all other hydrogen atoms were placed in calculated positions and refined in a “riding” model. For **15b**, the hydride position was not determined, all other hydrogen atoms were placed in calculated positions and refined in a “riding” model. The location and magnitude of the residual electron density was of no chemical significance.

Crystal data for **3e** (C₂₀H₃₂Cl₃NNbPSi): yellow (wedge), 0.14 × 0.22 × 0.22 mm, *M* = 530.80, orthorhombic, space group *Pbca*; *a* = 16.2130(3), *b* = 17.6513(4), *c* = 17.8176(4) Å; *a* = *b* = *γ* = 90°; *V* = 5099.1(2) Å³; *Z* = 8, ρ_{calc} = 1.38 g cm⁻³. Data collection: *T* = 150 K, μ = 0.90 mm⁻¹, λ = 0.71070 Å, $2\theta_{\text{max}}$ = 55.0°, 11 564 measured reflections, 5840 unique, 248 parameters, *R*₁ = 0.096, *wR*₂ = 0.0971 (3343 observed reflections with *I* ≥ 3 σ (*I*)), and *R*₁ = 0.1488 and *wR*₂ = 0.1404 (all data), GOOF = 1.03. The largest peak in the final difference Fourier map had an electron density of 1.87 e Å⁻³ and the lowest hole was of –0.98 e Å⁻³.

Crystal data for **3g** (C₂₆H₃₉NNbPSi): brown-yellow (block), 0.08 × 0.14 × 0.14 mm; *M* = 517.55; orthorhombic, space group *Pca*2₁; *a* = 17.2632(4), *b* = 9.2235(2), *c* = 17.0060(4) Å; $\alpha = \beta = \gamma = 90^\circ$; *V* = 2707.93(11) Å³; *Z* = 4, $\rho_{\text{calc}} = 1.269 \text{ g cm}^{-3}$. Data collection: *T* = 150 K, $\mu = 0.56 \text{ mm}^{-1}$, $\lambda = 0.71070 \text{ \AA}$, $2\theta_{\text{max}} = 54.96^\circ$, 19580 measured reflections, 5845 unique, 283 parameters, *R*₁ = 0.0361, *wR*₂ = 0.0755 (4981 observed reflections with *I* ≥ 2 $\theta(I)$), and *R*₁ = 0.0505 and *wR*₂ = 0.0814 (all data), *GOOF* = 1.067. The largest peak in the final difference Fourier map had an electron density of 0.942 e Å⁻³ and the lowest hole was of -0.606 e Å⁻³.

Crystal data for **15b** (C₂₃H₃₁CINNbPSi): dark green (block), 0.12 × 0.17 × 0.22 mm; *M* = 508.93; orthorhombic, space group *P2*₁2₁2₁; *a* = 8.3037(17), *b* = 13.897(3), *c* = 20.980(4) Å; $\alpha = \beta = \gamma = 90^\circ$; *V* = 2421.0(8) Å³; *Z* = 4, $\rho_{\text{calc}} = 1.396 \text{ g cm}^{-3}$. Data collection: *T* = 150 K, $\mu = 0.732 \text{ mm}^{-1}$, $\lambda = 0.71070 \text{ \AA}$, $2\theta_{\text{max}} = 54.96^\circ$, 23491 measured reflections, 5442 unique, 254 parameters, *R*₁ = 0.0384, *wR*₂ = 0.0381 (4300 observed reflections with *I* ≥ 3 $\theta(I)$), and *R*₁ = 0.0586 and *wR*₂ = 0.0543 (all data), *GOOF* = 1.102. The largest peak in the final difference Fourier map had an electron density of 0.64 e Å⁻³ and the lowest hole was of -0.59 e Å⁻³.

CCDC-636863 (for **3e**), CCDC-636864 (for **3g**) and CCDC-636865 (for **15b**) contain the supplementary crystallographic data for this paper. These data can be obtained free of charge from the Cambridge Crystallographic Data Centre via www.ccdc.cam.ac.uk/data_request/cif.

Acknowledgements

This work was supported through a Royal Society (London) joint research grant to GIN and PM, a YS INTAS fellowship and a RSC award for International Authors to GIN, a RFBR grant to SKI and AGR, and by a EPSRC award to SRD. GIN is also grateful to Brock University for further financial support.

- [1] a) D. S. Williams, M. H. Schofield, J. T. Anhaus, R. R. Schrock, *J. Am. Chem. Soc.* **1990**, *112*, 6728; b) D. S. Glueck, J. C. Green, R. I. Michelman, I. N. Wright, *Organometallics* **1992**, *11*, 4221; c) D. N. Williams, J. P. Mitchell, A. D. Pool, U. Siemeling, W. Clegg, D. C. R. Hockless, P. A. O'Neil, V. C. Gibson, *J. Chem. Soc. Dalton Trans.* **1992**, 739; d) D. S. Williams, M. H. Schofield, R. R. Schrock, *Organometallics* **1993**, *12*, 4560; e) J. Sundermeyer, D. Runge, *Angew. Chem.* **1994**, *106*, 1328; *Angew. Chem. Int. Ed. Engl.* **1994**, *33*, 1255; f) V. C. Gibson, *J. Chem. Soc. Dalton Trans.* **1994**, 1607; g) D. E. Wigley, *Prog. Inorg. Chem.* **1994**, *42*, 239.
- [2] a) G. J. P. Britovsek, V. C. Gibson, D. F. Wass, *Angew. Chem.* **1999**, *111*, 448; *Angew. Chem. Int. Ed.* **1999**, *38*, 428; b) V. C. Gibson, S. K. Spitzmesser, *Chem. Rev.* **2003**, *103*, 283; c) P. D. Bolton, P. Mountford, *Adv. Synth. Catal.* **2005**, *347*, 355.
- [3] a) J. Gavenonis, T. D. Tilley, *Organometallics* **2004**, *23*, 31; b) J. Gavenonis, T. D. Tilley, *Inorg. Chem.* **2004**, *43*, 4353; c) J. Gavenonis, T. D. Tilley, *Organometallics* **2002**, *21*, 5549; d) U. Burckhardt, G. L. Casty, J. Gavenonis, T. D. Tilley, *Organometallics* **2002**, *21*, 3108; e) I. Castillo, T. D. Tilley, *J. Organomet. Chem.* **2002**, *643–644*, 431; f) G. L. Casty, T. D. Tilley, G. P. A. Yap, A. L. Rheingold, *Organometallics* **1997**, *16*, 4746; g) T. I. Gountchev, T. D. Tilley, *J. Am. Chem. Soc.* **1997**, *119*, 12831.
- [4] A. H. Hoveyda, R. R. Schrock, *Chem. Eur. J.* **2001**, *7*, 945.
- [5] a) T. Chen, K. R. Sorasanne, Z. Wu, J. B. Diminnie, Z. Xue, *Inorg. Chim. Acta* **2003**, *345*, 113; b) Z. Wu, Z. Xue, *Organometallics* **2000**, *19*, 4191; c) L. H. McAlexander, M. Hung, L. Li, J. B. Diminnie, Z. Xue, G. P. A. Yap, A. L. Rheingold, *Organometallics* **1996**, *15*, 5231; d) Z. Xue, L. Li, L. K. Hoyt, J. B. Diminnie, J. L. Pollitte, *J. Am. Chem. Soc.* **1994**, *116*, 2169.
- [6] for example a) L. H. Gade, P. Mountford, *Coord. Chem. Rev.* **2001**, *216–217*, 65; b) P. Muller, C. Fruit, *Chem. Rev.* **2003**, *103*, 2905; c) N. Hazari, P. Mountford, *Acc. Chem. Res.* **2005**, *38*, 839; d) A. P. Duncan, R. G. Bergman, *Chem. Rec.* **2002**, *2*, 431; e) I. Bytschkov, S. Doye, *Eur. J. Org. Chem.* **2003**, 935.
- [7] a) U. Schubert, *Angew. Chem.* **1994**, *106*, 435; *Angew. Chem. Int. Ed. Engl.* **1994**, *33*, 419; b) M. Suginome, Y. Ito, *J. Chem. Soc., Dalton Trans.* **1998**, 1925; c) K. S. Hemant, K. H. Pannel, *Chem. Rev.* **1995**, *95*, 1351; d) S. Shimada, M. Tanaka, *Coord. Chem. Rev.* **2006**, *250*, 991.
- [8] Si–C activation/formation: a) C. E. F. Rickard, W. R. Roper, D. M. Salter, L. J. Wright, *Organometallics* **1992**, *11*, 3931; b) M. Aizenberg, D. Milstein, *J. Am. Chem. Soc.* **1995**, *117*, 6456; c) S. M. Maddock, C. E. F. Rickard, W. R. Roper, L. J. Wright, *Organometallics* **1996**, *15*, 1793; d) M. Okazaki, H. Tobita, H. Ogino, *J. Chem. Soc., Dalton Trans.* **1997**, 3531; e) D. Huang, R. H. Heyn, J. C. Bollinger, K. G. Caulton, *Organometallics* **1997**, *16*, 292; f) K. Ezbiansky, P. I. Djurovich, M. LaForest, D. J. Sinning, R. Zayes, D. H. Berry, *Organometallics* **1998**, *17*, 1455; g) I. Castillo, T. D. Tilley, *Organometallics* **2000**, *19*, 4733; h) I. Castillo, T. D. Tilley, *J. Am. Chem. Soc.* **2001**, *123*, 10526; i) I. Castillo, T. D. Tilley, *Organometallics* **2001**, *20*, 5598; j) T. Takao, M. Amako, H. Suzuki, *Organometallics* **2003**, *22*, 3855; k) V. K. Dioumaev, B. R. Yoo, L. J. Procopio, D. H. Berry, *J. Am. Chem. Soc.* **2003**, *125*, 8936; l) A. D. Sadow, T. D. Tilley, *Organometallics* **2003**, *22*, 3577; m) F. Ozawa, T. Tani, H. Katayama, *Organometallics* **2005**, *24*, 2511; n) M. W. Bouwkamp, E. Lobkovsky, P. J. Chirik, *J. Am. Chem. Soc.* **2005**, *127*, 9660; o) Y.-K. Sau, H.-K. Lee, I. D. Williams, W.-H. Leung, *Chem. Eur. J.* **2006**, *12*, 9323; p) M. Ingleson, H. Fa, n M. Peink, J. Tomaszewski, K. G. Caulton, *J. Am. Chem. Soc.* **2006**, *128*, 1804.
- [9] Selected publications on silane alcoholysis: a) J. Huhmann-Vincent, B. L. Scott, G. J. Kubas, *Inorg. Chim. Acta* **1999**, *294*, 240; b) X. Fang, J. Huhmann-Vincent, B. L. Scott, G. J. Kubas, *J. Organomet. Chem.* **2000**, *609*, 95; c) X. Fang, B. L. Scott, K. D. John, G. J. Kubas, *Organometallics* **2000**, *19*, 4141; d) E. Scharrer, S. Chang, M. Brookhart, *Organometallics* **1995**, *14*, 5686; e) U. Schubert, C. Lorenz, *Inorg. Chem.* **1997**, *36*, 1258; f) C. Lorenz, U. Schubert, *Chem. Ber.* **1995**, *130*, 1267; g) T. C. Bedard, J. Y. Corey, *J. Organomet. Chem.* **1992**, *428*, 315; h) E. Matarasso-Tchiroukhine, *J. Chem. Soc. Chem. Commun.* **1990**, 681; i) C. Egger, U. Schubert, *Z. Naturforsch., B: Chem. Sci.* **1991**, *46*, 783; j) X. Luo, R. H. Crabtree, *J. Am. Chem. Soc.* **1989**, *111*, 2527.
- [10] Only a few examples of silane additions to an imido group are known: a) U. Burckhardt, G. L. Casty, T. D. Tilley, T. W. Woo, U. Rothlisberger, *Organometallics* **2000**, *19*, 3830; b) For an apparent silyl migration to an imido group see: T. M. Cameron, C. G. Ortiz, I. Ghiviriga, K. A. Abboud, J. M. Boncella, *J. Am. Chem. Soc.* **2002**, *124*, 922–923; c) For related silane addition to a bridging nitrido ligand see: d) M. D. Fryzuk, B. A. MacKay, B. O. Patrick, *J. Am. Chem. Soc.* **2003**, *125*, 3234; e) For Si–N bond activation by a zirconium imido compound see: R. G. Howe, C. S. Tredget, S. C. Lawrence, S. Subongkoj, A. R. Cowley, P. Mountford, *Chem. Commun.* **2006**, 223.
- [11] T. E. Hanna, E. Lobkovsky, P. Chirik, *Eur. J. Inorg. Chem.* **2007**, *46*, 2359–2361.
- [12] J. J. Kennedy-Smith, K. A. Nolin, H. P. Gunterman, F. D. Toste, *J. Am. Chem. Soc.* **2003**, *125*, 4056–4057.
- [13] G. Du, P. E. Fanwick, M. M. Abu-Omar, *J. Am. Chem. Soc.* **2007**, *129*, 5180–5187.
- [14] a) G. I. Nikonov, L. G. Kuzmina, S. F. Vyboishchikov, D. A. Lemenovskii, J. A. K. Howard, *Chem. Eur. J.* **1999**, *5*, 2497; b) V. I. Bakmutov, J. A. K. Howard, D. A. Keen, L. G. Kuzmina, M. A. Leech, G. I. Nikonov, E. V. Vorontsov, C. C. Wilson, *J. Chem. Soc. Dalton Trans.* **2000**, 1631; c) G. I. Nikonov, L. G. Kuzmina, J. A. K. Howard, *J. Chem. Soc. Dalton Trans.* **2002**, 3037; d) K. Yu. Dorogov, E. Dumont, N.-N. Ho, A. V. Churakov, L. G. Kuzmina, J.-M. Poblet, A. J. Schultz, J. A. K. Howard, R. Bau, A. Lledos, G. I. Nikonov, *Organometallics* **2004**, *23*, 2845; e) K. U. Dorogov, M. Yousufuddin, N.-N. Ho, A. V. Churakov, L. G. Kuzmina, A. J. Schultz, S. A. Mason, J. A. K. Howard, D. A. Lemenovskii, R. Bau, G. I. Nikonov, *Inorg. Chem.* **2007**, *46*, 147.
- [15] S. K. Ignatov, N. H. Rees, B. R. Tyrrell, S. R. Dubberley, A. G. Razuvaev, P. Mountford, G. I. Nikonov, *Chem. Eur. J.* **2004**, *10*, 4991.

- [16] G. I. Nikonov, A. V. Churakov, L. G. Kuzmina, M. Y. Antipin, *Organometallics* **2003**, *22*, 2178.
- [17] a) A. D. Poole, V. C. Gibson, W. Clegg, *J. Chem. Soc. Chem. Commun.* **1992**, 237; b) U. Siemeling, V. C. Gibson, *J. Organomet. Chem.* **1992**, *426*, C25; c) J. K. Cockcroft, V. C. Gibson, J. A. K. Howard, A. D. Poole, U. Siemeling, C. Wilson, *J. Chem. Soc. Chem. Commun.* **1992**, 1668.
- [18] G. I. Nikonov, P. Mountford, S. K. Ignatov, J. C. Green, P. A. Cooke, M. A. Leech, L. G. Kuzmina, A. G. Razuvaev, N. H. Rees, A. J. Blake, J. A. K. Howard, D. A. Lemenovskii, *J. Chem. Soc., Dalton Trans.* **2001**, 2903.
- [19] Several d⁰ silylamido agostic complexes are known: a) W. A. Herrmann, N. W. Huberand, J. Behm, *Chem. Ber.* **1992**, *125*, 1405; b) L. J. Procopio, P. J. Carroll, D. H. Berry, *J. Am. Chem. Soc.* **1994**, *116*, 177; c) W. A. Herrmann, J. Eppinger, M. Spiegler, O. Runte, R. Anwender, *Organometallics* **1997**, *16*, 1813; d) I. Nagl, W. Scherer, M. Tafipolsky, R. Anwender, *Eur. J. Inorg. Chem.* **1999**, 1405; e) J. Eppinger, M. Spiegler, W. Hieringer, W. A. Herrmann, R. Anwender, *J. Am. Chem. Soc.* **2000**, *122*, 3080.
- [20] S. K. Ignatov, N. H. Rees, S. R. Dubberley, A. G. Razuvaev, P. Mountford, G. I. Nikonov, *Chem. Commun.* **2004**, 952.
- [21] Recent reviews on nonclassical Si–H interactions: a) G. J. Kubas, “Metal Dihydrogen and σ -Bond Complexes” Kluwer Academic/Plenum: New York **2001**; b) R. H. Crabtree, *Angew. Chem. Int. Ed. Engl.* **1993**, *32*, 789; c) J. Y. Corey, J. Braddock-Wilking, *Chem. Rev.* **1999**, *99*, 175; d) Z. Lin, *Chem. Soc. Rev.* **2002**, *31*, 239; e) G. I. Nikonov, *Adv. Organomet. Chem.* **2005**, *53*, 217.
- [22] G. I. Nikonov, P. Mountford, S. R. Dubberley, *Inorg. Chem.* **2003**, *42*, 258.
- [23] Other transition metal imido silyl complexes are known: a) U. Burckhardt, T. D. Tilley, *J. Am. Chem. Soc.* **1999**, *121*, 6328; b) refs. [3] and [5].
- [24] More in-depth discussion of the spectroscopic features of agostic complexes is added to Supporting Information.
- [25] a) For the related hydride imido complex Cp₂Nb(=NtBu)H the poorly observable hydride resonates at 3.17 ppm: A. N. Chernega, M. L. H. Green, A. G. Suarez, *J. Chem. Soc., Dalton Trans.* **1993**, 3031; b) d⁰ Hydride imido complex of Ta exhibits hydride resonance at 15.28 ppm: ref 3a.
- [26] a) M. D. Curtis, L. G. Bell, W. M. Butler, *Organometallics* **1985**, *4*, 701; b) J. Arnold, T. D. Tilley, A. L. Rheingold, S. J. Geib, *Organometallics* **1987**, *6*, 473; c) A. Antiñolo, F. Carrillo, M. Fajardo, A. Otero, M. Lanfranchi, M. A. Pellinghelli, *Organometallics* **1995**, *14*, 1518; d) G. I. Nikonov, L. G. Kuzmina, J. A. K. Howard, *J. Chem. Soc. Dalton Trans.* **2002**, 3037.
- [27] Signals of all magnetically active nuclei directly bound to niobium are severely broaden, and in some cases not observable, because of the high spin (9/2) of ⁹⁶Nb: a) J. A. Labinger, in *Comprehensive Organometallic Chemistry*, Vol. 3, R. W. Able, G. Wilkinson, F. G. A. Stone, Eds.; Pergamon, **1983**; b) V. I. Bakhmutov, E. V. Vorontsov, G. I. Nikonov, D. A. Lemenovskii, *Inorg. Chem.* **1998**, *37*, 279; c) In **3** this effect is increased relatively **2** because both the silyl and hydride ligands interact stronger with the metal through 2c–2e bonds.
- [28] S. R. Dubberley, S. K. Ignatov, N. H. Rees, A. G. Razuvaev, P. Mountford, G. I. Nikonov, *J. Am. Chem. Soc.* **2003**, *125*, 642.
- [29] K. Y. Dorogov, A. V. Churakov, L. G. Kuzmina, J. A. K. Howard, G. I. Nikonov, *Eur. J. Inorg. Chem.* **2004**, 771.
- [30] IHI consists of electron density transfer from the electron-rich metal-hydride bond on the antibonding σ^* (Si–X) orbital of the *trans* Si–X bond, leading to the elongation of M–H bond, the contraction of M–Si bond, and the elongation of Si–X bond (refs. [14–16, 18, 28]).
- [31] a) J. Arnold, T. D. Tilley, A. L. Rheingold, S. J. Geib, *Organometallics* **1987**, *6*, 473; b) Complex Cp₂Nb(SiCl₃)₂H is classical but has short Nb–Si bonds (2.5597(5) and 2.5776(5) Å), owing to the presence of three electron-withdrawing chlorine groups at Si (ref. [26]).
- [32] The connectivity of this complex has been established but the overall accuracy of this structure was low due to the poor quality of the crystal (ref. [18]).
- [33] J.-K. F. Buijink, J. H. Teuben, H. Kooijman, A. L. Spek, *Organometallics* **1994**, *13*, 2922.
- [34] J. Nieman, J. H. Teuben, J. C. Huffman, K. G. Caulton, *J. Organomet. Chem.* **1983**, *255*, 193.
- [35] a) A. M. Andreu, F. A. Jalon, A. Otero, P. Royo, A. A. M. Lanfredi, A. Tiripicchio, *J. Chem. Soc., Dalton Trans.* **1987**, 953; b) related X-ray characterized dppe complex: J. C. Daran, K. Prout, A. de Cian, M. L. H. Green, N. Sigantoria, *J. Organomet. Chem.* **1977**, *136*, C4; c) related Ta complex: V. C. Gibson, T. P. Kee, W. Clegg, *J. Chem. Soc., Dalton Trans.* **1990**, 3199.
- [36] a) C. C. Cummins, S. M. Baxter, P. T. Wolczanski, *J. Am. Chem. Soc.* **1988**, *110*, 8731; b) C. C. Cummins, C. P. Schaller, G. D. Van Duyne, P. T. Wolczanski, E. A.-W. Chan, R. Hoffmann, *J. Am. Chem. Soc.* **1991**, *113*, 2985; c) C. P. Schaller, P. T. Wolczanski, *Inorg. Chem.* **1993**, *32*, 131; d) T. R. Cundari, T. R. Klinckman, P. T. Wolczanski, *J. Am. Chem. Soc.* **2002**, *124*, 1481.
- [37] a) P. J. Walsh, F. J. Hollander, R. G. Bergman, *J. Am. Chem. Soc.* **1988**, *110*, 8729; b) P. J. Walsh, P. J. Baranger, R. G. Bergman, *J. Am. Chem. Soc.* **1992**, *114*, 1708.
- [38] See the Supporting Information for details.
- [39] Addition of the silane to **22** goes barrierlessly on the potential energy surface, so that the TS₂₂₋₁₉ cannot be found by standard methods. However, we found a transition state TS’₂₂₋₁₉ with the structural characteristics of a η^1 -silane complex, having electronic energy of 27.1 kcal mol⁻¹ ($\Delta G = 24.0$ kcal mol⁻¹), which is below the energy of the pair **22**+HSiClMe₂. This suggests that the initial attack of HSiClMe₂ on **22** most likely goes via a η^1 -silane intermediate Cp(MeN=)Nb(PMe₃)(η^1 -HSiClMe₂) which then rearranges via the TS’₂₂₋₁₉ to complex **19**.
- [40] For a recent example of such X→M stabilization see: H. Zhao, A. Ariafard, Z. Lin, *Organometallics* **2006**, *25*, 812.
- [41] F. H. Allen, O. Kennard, *Chem. Des. Autom. News* **1993**, *8*, 31.
- [42] U. Schubert, *Adv. Organomet. Chem.* **1990**, *30*, 151.
- [43] S. C. Dunn, N. Hazari, N. M. Jones, A. G. Moody, A. J. Blake, A. R. Cowley, J. C. Green, P. Mountford, *Chem. Eur. J.* **2005**, *11*, 2111.
- [44] A. Schorm, J. Sundermeyer, *Eur. J. Inorg. Chem.* **2001**, 2947.
- [45] Silane σ -bond metathesis reactions on imido complexes have been intensively studied by Tilley and co-workers: ref. [3a,b,d,e–g].
- [46] J. A. Pople et al.; Gaussian 03, Revision C.02, Gaussian, Inc.: Wallingford CT, **2004**. The full reference is in the Supporting Information.
- [47] a) A. D. Becke, *J. Chem. Phys.* **1993**, *98*, 5648; b) J. P. Perdew, K. Burke, Y. Wang, *Phys. Rev. B* **1996**, *54*, 16533.
- [48] P. J. Hay, W. R. Wadt, *J. Chem. Phys.* **1985**, *82*, 299.
- [49] a) SHELXTL-Plus, Release 5.10, Bruker AXS Inc., Madison, Wisconsin (USA), **1997**; b) for complex **3e** the program CRYSTALS has been used for structural refinement: D. J. Watkin, C. K. Prout, J. R. Carruthers, P. W. Betteridge, R. I. Cooper, CRYSTALS, issue 11, Chemical Crystallography Laboratory: Oxford, UK, **2001**.
- [50] **Note added in proof:** The following recent paper on IHI is pertinent to this publication; H. Sakaba, T. Hirata, C. Kabuto, K. Kabuto, *J. Organomet. Chem.* **2007**, *692*, 402.

Received: February 16, 2007

Published online: September 26, 2007